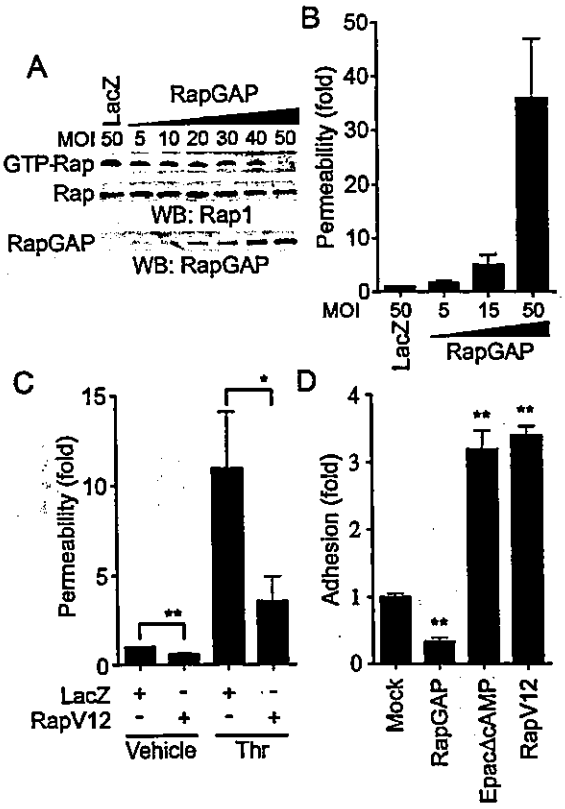

FIG. 8. Rap1 plays a critical role in VE-cadherin-dependent cell adhesion and endothelial barrier function. (A) Rap1 inactivation was assessed by detecting GTP-Rap1 in HUVECs infected with different MOI of adenovirus-expressing Rap1GAPII (RapGAP) as indicated at the top. An adenovirus-expressing LacZ at an MOI of 50 was used as a control. GTP-bound Rap1 (GTP-Rap) was detected by pull-down assay as described in Materials and Methods. Rap1 (Rap) and Rap1GAPII (RapGAP) expression were examined by Western blot analysis. (B) The permeability of FITC-dextran across HUVECs infected with adenovirus as indicated at the bottom was analyzed as described in Materials and Methods. Data are the means ± standard deviations of the results from three independent experiments and are expressed as increases relative to those of LacZ-infected cells. (C) Monolayer HUVECs infected with either an adenovirus-expressing LacZ or that expressing Rap1V12 at an MOI of 50 for 24 h were medium changed and cultured for another 24 h. The permeability of cells upon 2-U/ml thrombin stimulation (Thr) after starvation for 1 h was analyzed as described in the legend to Fig. 1B. Data are the means ± standard deviations of the results from five independent experiments and are expressed as inductions relative to those of untreated HUVECs infected with the LacZ-expressing virus. (D) HUVECs were transfected with either empty vector (Mock), plasmids expressing Rap1GAPII (RapGAP), EpacΔcAMP, or Rap1V12 together with the luciferase reporter construct. Transfected cells were plated on the VEC-Fc-coated dish and allowed to adhere for 15 min. Cell adhesion was analyzed as described in Materials and Methods. Data are expressed as increases compared to those of mock-transfected cells. The results indicate the means ± standard deviations of the results from triplicate samples. Similar results were obtained in three independent experiments. Significant differences between two groups in panel C or from the control in panel D are determined by Student's *t* test and are indicated by a single asterisk ($P < 0.05$) or double asterisks ($P < 0.01$).

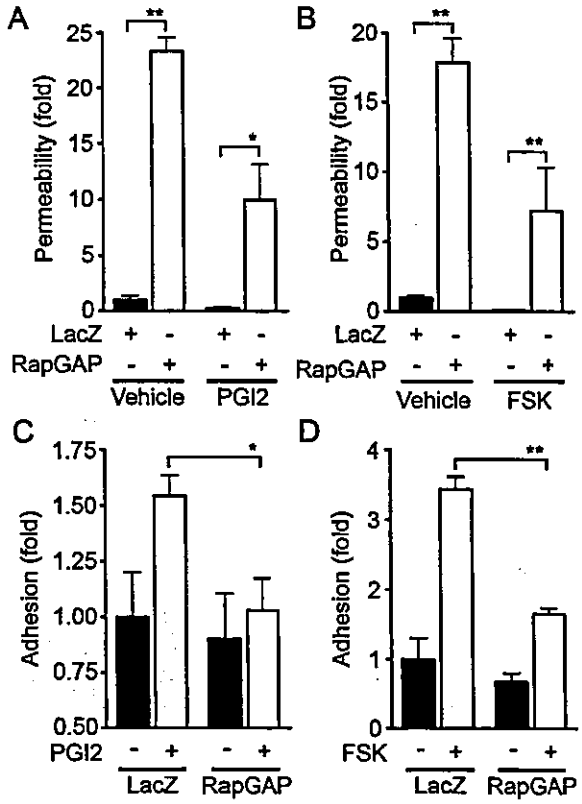

FIG. 9. Inactivation of Rap1 reduces PGI2- and FSK-induced barrier function and VE-cadherin-mediated cell adhesion. (A) Monolayer-cultured HUVECs grown on transwell filters were infected with either LacZ-expressing adenovirus (Ad-LacZ) or Rap1GAPII-expressing virus (Ad-RapGAP) at an MOI of 40 for 24 h. Medium was replaced with fresh medium after infection. Cells were cultured for an additional 24 h and treated with 10 μg of PGI2/ml for 30 min after serum starvation for 1 h. Permeability was analyzed as described in Materials and Methods. (B) The effect of 10 μM FSK on permeability in HUVECs infected with Ad-RapGAP was similarly analyzed. (C) HUVECs were infected with either Ad-LacZ or Ad-RapGAP at an MOI of 40 for 24 h. HUVECs resuspended in medium 199 with 0.5% BSA were plated onto VEC-Fc-coated dishes in the presence (+) or absence (−) of 10 μg of PGI2/ml for 7 min. Cell adhesion activity was quantified as described in the legend to Fig. 4A. (D) The effect of FSK on adhesion of HUVECs infected with Ad-RapGAP was analyzed similarly to that described for panel C. Resuspended HUVECs were preincubated with 10 μM FSK for 10 min before plating. Significant differences between two groups determined by Student's *t* test are indicated by a single asterisk ($P < 0.05$) or double asterisks ($P < 0.01$).

FSK, and 8-CPT-2′-O-Me-cAMP dramatically induced accumulation of polymerized actin and cortactin at cell-cell contacts (Fig. 10A). To explore the involvement of Rap1 in cAMP-mediated cortical actin rearrangement, an expression vector encoding Rap1GAPII was introduced into endothelial cells. FSK enhanced actin polymerization at cell-cell contacts in cells transfected with control vector encoding EGFP, whereas it did not in cells expressing Rap1GAPII (Fig. 10B). Cytochalasin D, an actin-depolymerizing agent, attenuated FSK-induced barrier enhancement (Fig. 10C) and inhibited FSK-induced VE-cadherin-dependent cell adhesion (Fig. 10D). These results suggest that the cortical actin rearrangement promoted by

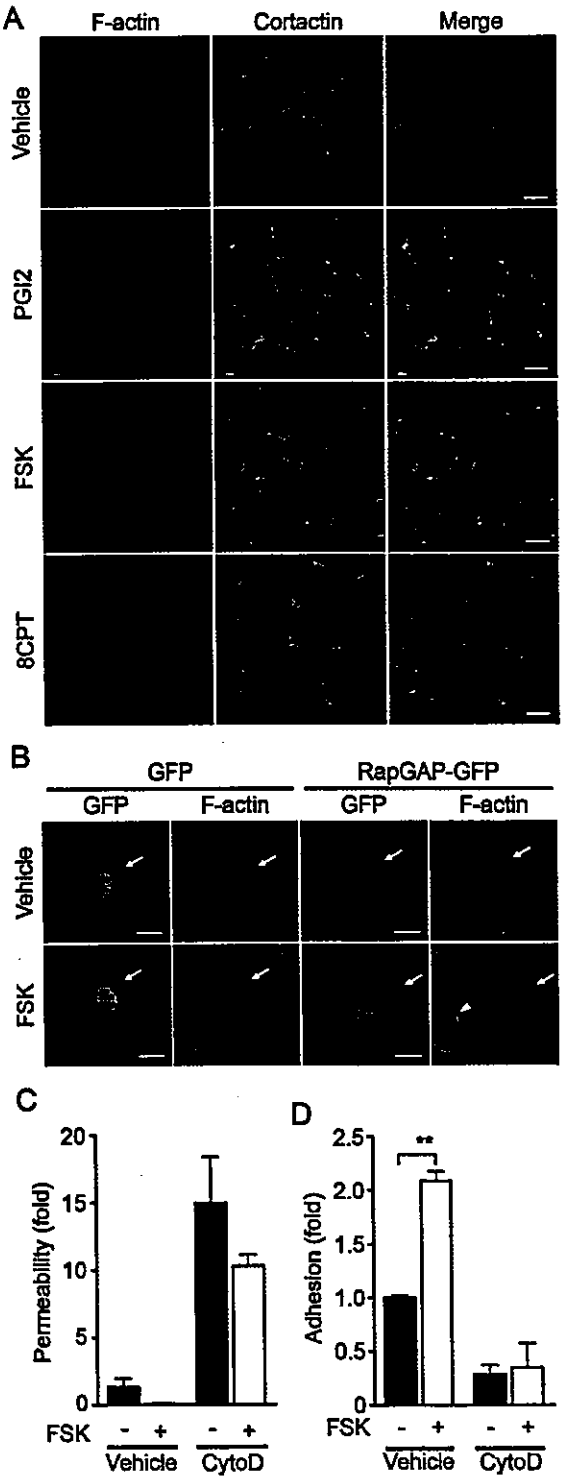

FIG. 10. cAMP induces cortical actin rearrangement in a Rap1-dependent manner. (A) Monolayer-cultured HUVECs starved in 0.5% BSA-containing medium 199 for 3 h were stimulated with vehicle (top row), 10-μg/ml PGI2 (second row), 10 μM FSK (third row), and 0.2 mM 8-CPT-2′-O-Me-cAMP (8CPT) (bottom row) for 30 min. Fixed and permeabilized cells were stained with rhodamine-phalloidin (left column) and with anti-cortactin (center column). Rhodamine images to detect F-actin (red) and Alexa 488 images for cortactin visualized by Alexa 488-labeled secondary antibody (green) were obtained through a confocal microscope (BX50WI). Right panels show the merged images of rhodamine and Alexa 488 images. Bars, 20 μm. (B) HUVECs transfected with an EGFP-expressing vector (left) and pCXN2-Rap1GAPII-IRES-EGFP (right) were serum starved in 0.5% BSA-containing medium 199 for 3 h and stimulated with vehicle (top panels) and 10 μM FSK (bottom panels). Cells were fixed, permeabilized, and stained with Rhodamine-phalloidin. EGFP images (green) and rhodamine images showing F-actin (red) were obtained similar to those in panel A. Arrows and arrowhead indicate transfected and untransfected cells, respectively. Bars, 20 μm. (C) Cell permeability of HUVECs pretreated with 2 μM cytochalasin D (CytoD) for 30 min followed by 10 μM FSK stimulation for 30 min was analyzed as described in the legend to Fig. 1A. −, absent; +, present. (D) The effect of pretreatment of 2 μM cytochalasin D (CytoD) on adhesion of HUVECs stimulated with FSK was analyzed as described in the legend to Fig. 5E. A significant difference between two groups determined by Student's t test is indicated by double asterisks ($P < 0.01$).

cAMP-Epac-Rap1 signaling may contribute to the potentiation of endothelial barrier function and VE-cadherin-dependent cell adhesion.

DISCUSSION

cAMP is a well-known intracellular signaling molecule that is capable of restoring diminished endothelial barrier function. Previous reports suggested that cAMP-induced barrier enhancement occurs through PKA (27, 39). In this study, however, we demonstrated a novel PKA-independent signaling pathway, the cAMP-Epac-Rap1 signaling pathway, involved in cAMP-induced barrier function based on the following observations. PGI2- and FSK-reduced endothelial permeability was insensitive to H89. A specific activator for Epac, 8-CPT-2′-O-Me-cAMP, reduced both basal and thrombin-increased permeability. Plasma leakage in response to VEGF was also inhibited by 8-CPT-2′-O-Me-cAMP in vivo. We found that the activation of Rap1 leads to decreased permeability. Not only all cAMP-elevating bio-ligands we tested but also FSK, db-cAMP, and IBMX activated Rap1. Consistently, cAMP-dependent Rap1 activation upon stimulation by these ligands involved Epac in the regulation of barrier function. A previous report showed that Rap1 is phosphorylated by PKA in neutrophils and platelets, although the function of phosphorylated Rap1 has not been elucidated (37). So far, Epac is known to regulate several biological functions including integrin-dependent cell adhesion, insulin secretion, and calcium release through ryanodine-sensitive Ca^{2+} channels (reviewed in reference 5). In addition to these Epac-mediated functions, we show, for the first time, that Epac-Rap1 signaling is important for regulation of endothelial barrier function.

AJ assembly contributes to the regulation of barrier function. Rap1 is involved in the formation and maintenance of AJ constituted by cadherin (23, 41). Recently, it has been reported that homophilic ligation of E-cadherin induced Rap1 activation, which may be responsible for maturation of AJ (20). Consistently, suppression of endogenous Rap1 inhibits formation of E-cadherin-dependent cell adhesion (36), suggesting the critical role of Rap1 in the establishment of cadherin-based cell-cell contacts. Here, we demonstrate that Rap1 also acts downstream of cAMP-Epac to potentiate VE-cadherin-depen-

dent cell adhesion, thereby improving barrier function. In addition to cAMP-elevating ligands, S1P, which enhances AJ formation and barrier function (18, 26), also activated Rap1 (our unpublished data). Thus, Rap1 may play a crucial role in barrier function induced by various types of barrier-improving factors.

Our data and previous studies show that cAMP protects thrombin-induced endothelial barrier dysfunction. cAMP does not limit the effect of thrombin on the initial loss of endothelial barrier (32). Instead, cAMP enhances the restoration of barrier function disrupted by thrombin. Recently, it was also reported that Cdc42 regulates the restoration of endothelial barrier function disrupted by thrombin (24). Thus, cAMP-Epac-Rap1 signaling may facilitate the formation of VE-cadherin-based cell-cell contacts, cooperatively or in parallel with Cdc42.

Rap1 enhances integrin-dependent cell adhesion in a variety of hematopoietic cells by modulating the affinity and avidity of integrin (6, 22). Cell adhesion to VEC-Fc-coated dishes was augmented by Rap1 activation, suggesting that the homophilic binding of VE-cadherin is also likely ascribed to the affinity and avidity of VE-cadherin modulated by Rap1-triggered inside out signaling. Hogan et al. reported that Rap1 activity is required for the targeting of E-cadherin molecules into nascent cell-cell contact sites, which in turn leads to the maturation of E-cadherin-based cell-cell contacts (20). Thus, cAMP-Epac-Rap1 signaling may also regulate the recruitment of VE-cadherin into maturing cell-cell contacts. Since downstream signaling of Rap1 that increases homophilic binding of VE-cadherin has not yet been characterized, the effector of cAMP-Epac-Rap1 signaling will need to be identified.

The actin cytoskeleton is a critical determinant of vascular integrity (10). PGI2, FSK, and 8-CPT-2'-O-Me-cAMP induced cortical actin rearrangement in a Rap1-dependent manner. FSK-induced VE-cadherin-dependent cell adhesion was inhibited by cytochalasin D. Thus, Rap1 may promote VE-cadherin-dependent cell adhesion by inducing cortical actin rearrangement. AF-6 may act downstream of Rap1 to regulate the actin cytoskeleton, since it binds to GTP-bound Rap1 and the actin cytoskeleton regulator, profilin, and is localized at AJ (2). Consistently, Canoe, the drosophila homolog of AF-6, and Rap1 function in the same molecular pathway during embryonic dorsal closure, which requires cell-cell contacts (3). S1P promotes endothelial barrier function by inducing Rac-dependent cortical actin rearrangement. S1P also induces Rap1 activation (our unpublished data). A previous report indicates that Rac can function downstream of Rap1 in the processing of the amyloid precursor protein (28). Taken together, Rac may act downstream of Rap1 to induce cortical actin rearrangement.

In conclusion, we have demonstrated that the cAMP-Epac-Rap1 signaling pathway promotes VE-cadherin-mediated cell adhesion and consequently improves endothelial barrier function.

ACKNOWLEDGMENTS

We thank J. L. Bos and W. A. Muller for plasmids, M. Matsuda and S. Hattori for adenovirus, J. T. Pearson for critical reading, and M. Sone, K. Yamamoto, and N. Irisawa for technical assistance.

This work was supported by grants from the Ministry of Health, Labor, and Welfare of Japan, from the Promotion of Fundamental Studies in Health Science of the Organization for Pharmaceutical Safety and Research of Japan, from the Ministry of Education, Science, Sports, and Culture of Japan, from the Uehara Memorial Foundation, and from Senri Life Science Foundation.

REFERENCES

1. **Andriopoulou, P., P. Navarro, A. Zanetti, M. G. Lampugnani, and E. Dejana.** 1999. Histamine induces tyrosine phosphorylation of endothelial cell-to-cell adherens junctions. Arterioscler. Thromb. Vasc. Biol. 19:2286–2297.
2. **Boettner, B., E. E. Govek, J. Cross, and L. Van Aelst.** 2000. The junctional multidomain protein AF-6 is a binding partner of the Rap1A GTPase and associates with the actin cytoskeletal regulator profilin. Proc. Natl. Acad. Sci. USA 97:9064–9069.
3. **Boettner, B., P. Harjes, S. Ishimaru, M. Heke, H. Q. Fan, Y. Qin, L. Van Aelst, and U. Gaul.** 2003. The AF-6 homolog canoe acts as a Rap1 effector during dorsal closure of the Drosophila embryo. Genetics 165:159–169.
4. **Bogatcheva, N. V., J. G. Garcia, and A. D. Verin.** 2002. Molecular mechanisms of thrombin-induced endothelial cell permeability. Biochemistry (Moscow) 67:75–84.
5. **Bos, J. L.** 2003. Epac: a new cAMP target and new avenues in cAMP research. Nat. Rev. Mol. Cell Biol. 4:733–738.
6. **Bos, J. L., J. de Rooij, and K. A. Reedquist.** 2001. Rap1 signalling: adhering to new models. Nat. Rev. Mol. Cell Biol. 2:369–377.
7. **Chijiwa, T., A. Mishima, M. Hagiwara, M. Sano, K. Hayashi, T. Inoue, K. Naito, T. Toshioka, and H. Hidaka.** 1990. Inhibition of forskolin-induced neurite outgrowth and protein phosphorylation by a newly synthesized selective inhibitor of cyclic AMP-dependent protein kinase, N-[2-(p-bromocinnamylamino)ethyl]-5-isoquinolinesulfonamide (H-89), of PC12D pheochromocytoma cells. J. Biol. Chem. 265:5267–5272.
8. **Daly, R. J.** 2004. Cortactin signalling and dynamic actin networks. Biochem. J. 382:13–25. [Online.] doi:10.1042/BJ20040737.
9. **Dejana, E.** 2004. Endothelial cell-cell junctions: happy together. Nat. Rev. Mol. Cell Biol. 5:261–270.
10. **Dudek, S. M., and J. G. Garcia.** 2001. Cytoskeletal regulation of pulmonary vascular permeability. J. Appl. Physiol. 91:1487–1500.
11. **Dudek, S. M., J. R. Jacobson, E. T. Chiang, K. G. Birukov, P. Wang, X. Zhan, and J. G. Garcia.** 2004. Pulmonary endothelial cell barrier enhancement by sphingosine 1-phosphate: roles for cortactin and myosin light chain kinase. J. Biol. Chem. 279:24692–24700.
12. **Endo, A., K. Nagashima, H. Kurose, S. Mochizuki, M. Matsuda, and N. Mochizuki.** 2002. Sphingosine 1-phosphate induces membrane ruffling and increases motility of human umbilical vein endothelial cells via vascular endothelial growth factor receptor and CrkII. J. Biol. Chem. 277:23747–23754.
13. **Enserink, J. M., A. E. Christensen, J. de Rooij, M. van Triest, F. Schwede, H. G. Genieser, S. O. Doskeland, J. L. Blank, and J. L. Bos.** 2002. A novel Epac-specific cAMP analogue demonstrates independent regulation of Rap1 and ERK. Nat. Cell Biol. 4:901–906.
14. **Esser, S., M. G. Lampugnani, M. Corada, E. Dejana, and W. Risau.** 1998. Vascular endothelial growth factor induces VE-cadherin tyrosine phosphorylation in endothelial cells. J. Cell Sci. 111(Pt 13):1853–1865.
15. **Farmer, P. J., S. G. Bernier, A. Lepage, G. Guillemette, D. Regoli, and P. Sirois.** 2001. Permeability of endothelial monolayers to albumin is increased by bradykinin and inhibited by prostaglandins. Am. J. Physiol. Lung Cell. Mol. Physiol. 280:L732–L738.
16. **Fukuhara, S., M. J. Marinissen, M. Chiariello, and J. S. Gutkind.** 2000. Signaling from G protein-coupled receptors to ERK5/Big MAPK 1 involves Galpha q and Galpha 12/13 families of heterotrimeric G proteins. Evidence for the existence of a novel Ras AND Rho-independent pathway. J. Biol. Chem. 275:21730–21736.
17. **Gamble, J. R., J. Drew, L. Trezise, A. Underwood, M. Parsons, L. Kasminkas, J. Rudge, G. Yancopoulos, and M. A. Vadas.** 2000. Angiopoietin-1 is an antipermeability and anti-inflammatory agent in vitro and targets cell junctions. Circ. Res. 87:603–607.
18. **Garcia, J. G., F. Liu, A. D. Verin, A. Birukova, M. A. Dechert, W. T. Gerthoffer, J. R. Bamberg, and D. English.** 2001. Sphingosine 1-phosphate promotes endothelial cell barrier integrity by Edg-dependent cytoskeletal rearrangement. J. Clin. Investig. 108:689–701.
19. **Hippenstiel, S., M. Witzenrath, B. Schmeck, A. Hocke, M. Krisp, M. Krull, J. Seybold, W. Seeger, W. Rascher, H. Schutte, and N. Suttorp.** 2002. Adrenomedullin reduces endothelial hyperpermeability. Circ. Res. 91:618–625.
20. **Hogan, C., N. Serpente, P. Cogram, C. R. Hosking, C. U. Bialucha, S. M. Feller, V. M. M. Braga, W. Birchmeier, and Y. Fujita.** 2004. Rap1 regulates the formation of E-cadherin-based cell-cell contacts. Mol. Cell. Biol. 24: 6690–6700.
21. **Kawasaki, H., G. M. Springett, N. Mochizuki, S. Toki, M. Nakaya, M. Matsuda, D. E. Housman, and A. M. Graybiel.** 1998. A family of cAMP-binding proteins that directly activate Rap1. Science 282:2275–2279.
22. **Kinbara, K., L. E. Goldfinger, M. Hansen, F. L. Chou, and M. H. Ginsberg.**

2003. Ras GTPases: integrins' friends or foes? Nat. Rev. Mol. Cell Biol. 4:767–776.
23. **Knox, A. L., and N. H. Brown.** 2002. Rap1 GTPase regulation of adherens junction positioning and cell adhesion. Science 295:1285–1288.
24. **Kouklis, P., M. Konstantoulaki, S. Vogel, M. Broman, and A. B. Malik.** 2004. Cdc42 regulates the restoration of endothelial barrier function. Circ. Res. 94:159–166.
25. **Langeler, E. G., and V. W. van Hinsbergh.** 1991. Norepinephrine and iloprost improve barrier function of human endothelial cell monolayers: role of cAMP. Am. J. Physiol. 260:C1052–C1059.
26. **Lee, M. J., S. Thangada, K. P. Claffey, N. Ancellin, C. H. Liu, M. Kluk, M. Volpi, R. I. Sha'afi, and T. Hla.** 1999. Vascular endothelial cell adherens junction assembly and morphogenesis induced by sphingosine-1-phosphate. Cell 99:301–312.
27. **Lum, H., H. A. Jaffe, I. T. Schulz, A. Masood, A. RayChaudhury, and R. D. Green.** 1999. Expression of PKA inhibitor (PKI) gene abolishes cAMP-mediated protection to endothelial barrier dysfunction. Am. J. Physiol. 277: C580–C588.
28. **Maillet, M., S. J. Robert, M. Cacquevel, M. Gastineau, D. Vivien, J. Bertoglio, J. L. Zugaza, R. Fischmeister, and F. Lezoualc'h.** 2003. Crosstalk between Rap1 and Rac regulates secretion of sAPPalpha. Nat. Cell Biol. 5:633–639.
29. **Miles, A. A., and E. M. Miles.** 1952. Vascular reactions to histamine, histamine-liberator and leukotaxine in the skin of guinea-pigs. J. Physiol. 118: 228–257.
30. **Mochizuki, N., Y. Ohba, E. Kiyokawa, T. Kurata, T. Murakami, T. Ozaki, A. Kitabatake, K. Nagashima, and M. Matsuda.** 1999. Activation of the ERK/MAPK pathway by an isoform of rap1GAP associated with G alpha(i). Nature 400:891–894.
31. **Mori, Y., T. Nishikimi, N. Kobayashi, H. Ono, K. Kangawa, and H. Matsuoka.** 2002. Long-term adrenomedullin infusion improves survival in malignant hypertensive rats. Hypertension 40:107–113.
32. **Moy, A. B., J. E. Bodmer, K. Blackwell, S. Shasby, and D. M. Shasby.** 1998. cAMP protects endothelial barrier function independent of inhibiting MLC20-dependent tension development. Am. J. Physiol. 274:L1024–L1029.
33. **Navarro, P., L. Ruco, and E. Dejana.** 1998. Differential localization of VE- and N-cadherins in human endothelial cells: VE-cadherin competes with N-cadherin for junctional localization. J. Cell Biol. 140:1475–1484.
34. **Ohba, Y., K. Ikuta, A. Ogura, J. Matsuda, N. Mochizuki, K. Nagashima, K. Kurokawa, B. J. Mayer, K. Maki, J. Miyazaki, and M. Matsuda.** 2001. Requirement for C3G-dependent Rap1 activation for cell adhesion and embryogenesis. EMBO J. 20:3333–3341.
35. **Parandoosh, Z., C. A. Bogowitz, and M. P. Nova.** 1998. A fluorometric assay for the measurement of endothelial cell density in vitro. In Vitro Cell. Dev. Biol. Anim. 34:772–776.
36. **Price, L. S., A. Hajdo-Milasinovic, J. Zhao, F. J. Zwartkruis, J. G. Collard, and J. L. Bos.** 2004. Rap1 regulates E-cadherin-mediated cell-cell adhesion. J. Biol. Chem. 279:35127–35132.
37. **Quilliam, L. A., H. Mueller, B. P. Bohl, V. Prossnitz, L. A. Sklar, C. J. Der, and G. M. Bokoch.** 1991. Rap1A is a substrate for cyclic AMP-dependent protein kinase in human neutrophils. J. Immunol. 147:1628–1635.
38. **Shaywitz, A. J., and M. E. Greenberg.** 1999. CREB: a stimulus-induced transcription factor activated by a diverse array of extracellular signals. Annu. Rev. Biochem. 68:821–861.
39. **Stelzner, T. J., J. V. Weil, and R. F. O'Brien.** 1989. Role of cyclic adenosine monophosphate in the induction of endothelial barrier properties. J. Cell. Physiol. 139:157–166.
40. **Ukropec, J. A., M. K. Hollinger, S. M. Salva, and M. J. Woolkalis.** 2000. SHP2 association with VE-cadherin complexes in human endothelial cells is regulated by thrombin. J. Biol. Chem. 275:5983–5986.
41. **Yajnik, V., C. Paulding, R. Sordella, A. L. McClatchey, M. Saito, D. C. Wahrer, P. Reynolds, D. W. Bell, R. Lake, S. van den Heuvel, J. Settleman, and D. A. Haber.** 2003. DOCK4, a GTPase activator, is disrupted during tumorigenesis. Cell 112:673–684.
42. **Yano, H., Y. Mazaki, K. Kurokawa, S. K. Hanks, M. Matsuda, and H. Sabe.** 2004. Roles played by a subset of integrin signaling molecules in cadherin-based cell-cell adhesion. J. Cell Biol. 166:283–295.
43. **Yuan, S. Y.** 2002. Protein kinase signaling in the modulation of microvascular permeability. Vascul. Pharmacol. 39:213–223.

Effects of Ghrelin Administration on Left Ventricular Function, Exercise Capacity, and Muscle Wasting in Patients With Chronic Heart Failure

Noritoshi Nagaya, MD; Junji Moriya, MD; Yoshio Yasumura, MD; Masaaki Uematsu, MD; Fumiaki Ono, MD; Wataru Shimizu, MD; Kazuyuki Ueno, PhD; Masafumi Kitakaze, MD; Kunio Miyatake, MD; Kenji Kangawa, PhD

Background—Ghrelin is a novel growth hormone–releasing peptide that also induces vasodilation, inhibits sympathetic nerve activity, and stimulates feeding through growth hormone–independent mechanisms. We investigated the effects of ghrelin on left ventricular (LV) function, exercise capacity, and muscle wasting in patients with chronic heart failure (CHF).

Methods and Results—Human synthetic ghrelin (2 μg/kg twice a day) was intravenously administered to 10 patients with CHF for 3 weeks. Echocardiography, cardiopulmonary exercise testing, dual x-ray absorptiometry, and blood sampling were performed before and after ghrelin therapy. A single administration of ghrelin elicited a marked increase in serum GH (25-fold). Three-week administration of ghrelin resulted in a significant decrease in plasma norepinephrine (1132±188 to 655±134 pg/mL; $P<0.001$). Ghrelin increased LV ejection fraction (27±2% to 31±2%; $P<0.05$) in association with an increase in LV mass and a decrease in LV end-systolic volume. Treatment with ghrelin increased peak workload and peak oxygen consumption during exercise. Ghrelin improved muscle wasting, as indicated by increases in muscle strength and lean body mass. These parameters remained unchanged in 8 patients with CHF who did not receive ghrelin therapy.

Conclusions—These preliminary results suggest that repeated administration of ghrelin improves LV function, exercise capacity, and muscle wasting in patients with CHF. (***Circulation.*** **2004;110:3674-3679.)**

Key Words: growth substances ■ heart failure ■ hormones ■ nutrition

Left ventricular (LV) remodeling (dilatation and wall thinning) and cardiac cachexia (body weight loss and muscle wasting) often are observed in patients with end-stage chronic heart failure (CHF).[1,2] Growth hormone (GH) and its mediator, insulinlike growth factor-1 (IGF-1), are anabolic hormones that are essential for skeletal and myocardial growth and metabolic homeostasis.[3,4] Earlier studies have shown that GH supplementation may have beneficial effects on LV myocardial structure and function in some patients with CHF,[5] although the importance of GH resistance[6] and neutral results of randomized trials also have been reported.[7,8]

Ghrelin is a novel GH-releasing peptide that was isolated from the stomach and has been identified as an endogenous ligand for the growth hormone secretagogue receptor.[9] Therefore, we believed that administration of ghrelin may induce beneficial changes in LV function and energy metabolism in patients with CHF via a GH-dependent mechanism. On the other hand, growth hormone secretagogue receptor mRNA is detected not only in the hypothalamus and pituitary but also in the heart and blood vessels,[10] implying direct cardiovascular effects of ghrelin. Wiley and Davenport[11] have demonstrated that ghrelin is an endothelium-independent vasodilator in isolated human arteries. We have shown that intravenous administration of ghrelin decreases systemic vascular resistance and increases cardiac output in patients with CHF.[12] Furthermore, ghrelin induces a positive energy balance by stimulating food intake[13,14] and adiposity[15] through GH-independent mechanisms. These findings raise the possibility that ghrelin administration may have beneficial effects in cachectic patients with CHF. In fact, we recently have demonstrated that treatment with ghrelin improves not only LV function but also cardiac cachexia in rats with CHF.[16] In humans, however, the potential effects of ghrelin as a therapeutic agent for CHF remain unknown.

Thus, the purposes of this study were as follows: (1) to investigate whether repeated administration of ghrelin im-

Received April 30, 2004; revision received July 6, 2004; accepted August 23, 2004.

From the Department of Internal Medicine, National Cardiovascular Center, Osaka (N.N., J.M., Y.Y., F.O., W.S., M.K., K.M.); Cardiovascular Division, Kansai Rosai Hospital, Hyogo (M.U.); and Departments of Pharmacy (K.U.) and Biochemistry (K.K.), National Cardiovascular Center Research Institute, Osaka, Japan.

Reprint requests to Noritoshi Nagaya, MD, Department of Internal Medicine, National Cardiovascular Center, 5-7-1 Fujishirodai, Suita, Osaka 565-8565, Japan. E-mail nagayann@hsp.ncvc.go.jp

Circulation is available at http://www.circulationaha.org

DOI: 10.1161/01.CIR.0000149746.62908.BB

TABLE 1. Patient Characteristics

	Control Group (n=8)	Ghrelin Group (n=10)
Age, y	74±2	75±2
Sex, M/F	6/2	7/3
Body mass index, kg/m²	19.0±1.1	19.0±0.9
Cause of CHF, n		
Dilated cardiomyopathy	4	4
Ischemic cardiomyopathy	1	3
Hypertensive heart disease	2	1
Valvular heart disease	1	2
NYHA functional class, n		
III	8	9
IV	0	1
LVEF, %	28±2	27±2
Presence of cardiac cachexia, n	6	8
Medication use, n		
Digoxin	6	9
ACE inhibitors	7	9
A II blockers	2	2
β-Blockers	6	7
Diuretics	7	10

LVEF indicates LV ejection fraction; A II, angiotensin II. Data are mean±SEM.

proves LV myocardial structure and function in patients with CHF, (2) to examine whether ghrelin improves exercise capacity in such patients, and (3) to examine whether ghrelin induces anabolic effects in patients with CHF.

Methods

Study Subjects

Eighteen patients with CHF (13 men, 5 women; mean age, 75 years; range, 63 to 80 years) were included in this study. Inclusion criteria were as follows: (1) LV ejection fraction <35% as assessed by cardiac catheterization, (2) a stable clinical condition, and (3) clinical evidence of heart failure despite conventional therapy. Exclusion criteria were the presence of any of the following: (1) chronic renal impairment (serum creatinine level ≥2.0 mg/dL), (2) significant liver dysfunction, (3) evidence of malignant diseases, (4) active infection, (5) hematologic abnormalities, or (6) systolic blood pressure <90 mm Hg. Ten patients with CHF (ghrelin group) received repeated administrations of ghrelin. Although this study was neither randomized nor placebo controlled, 8 patients with CHF who did not receive ghrelin (control group) were studied to exclude time-course effects during hospitalization. Patients in the ghrelin group were admitted only for the study. Those in the control group had been in hospital for diagnostic examination and stayed for 3 weeks for the study. There was no significant difference in demographic, clinical, or hemodynamic data at baseline between the ghrelin and control groups (Table 1). Eight patients in the ghrelin group and 6 patients in the control group were defined as exhibiting cardiac cachexia, as reported previously.[17] The weight loss in cachectic patients amounted to 6.4±0.4 kg or 11.8±0.7% loss of previous body weight during 14±2 months. The ethics committee of the National Cardiovascular Center approved the study, and all patients gave written informed consent.

Preparation of Human Ghrelin

Human synthetic ghrelin was obtained from the Peptide Institute Inc. This peptide is not commercially available. Ghrelin was dissolved in distilled water with 4% D-mannitol and sterilized by passage through a 0.22-μm filter (Millipore Co). Ghrelin was stored in 2-mL volumes, each containing 200 μg ghrelin. The chemical nature and content of the human ghrelin in vials were verified by high-performance liquid chromatography and radioimmunoassay. All vials were stored frozen at −80°C from the time of dispensing until the time of preparation for administration.

Study Protocol

This study was performed while patients were in a stable clinical condition during hospitalization. Ghrelin (2 μg/kg, 10 mL solution) was administered intravenously over 30 minutes at a constant rate. The infusion was repeated twice a day (before breakfast and before dinner) for 3 weeks. Study patients in both groups remained hospitalized for 3 weeks. Echocardiography, cardiopulmonary exercise testing, dual x-ray absorptiometry, hand-grip test, and blood sampling were performed at baseline and after 3 weeks of treatment with ghrelin (ghrelin group) or without ghrelin (control group). Long-term medication, including digitalis, diuretics, ACE inhibitors, and β-blockers, was kept constant during this study protocol.

Echocardiographic Studies

Echocardiography was performed by an investigator blinded to treatment allocation. Two-dimensional targeted M-mode tracings were obtained at the level of the papillary muscles with an echocardiographic system equipped with a 3.5-MHz sector scan probe (SONOS 2000, Hewlett Packard). LV wall thickness, dimensions, and fractional shortening were measured according to the recommendations of the American Society of Echocardiology from at least 3 consecutive cardiac cycles. LV end-diastolic volume, end-systolic volume, and ejection fraction were calculated with a modified version of Simpson's method.[18]

Cardiopulmonary Exercise Testing

Cardiopulmonary exercise testing was performed in all patients except 1, who underwent a 6-minute walk test as recommended by attending physicians. The patients exercised seated on a cycle ergometer. The work rate was then increased by 15 W/min up to their symptom-limited maximum. Breath-by-breath gas analysis was performed with an AE280 (Minato Medical Science).[19] Exercise capacity was evaluated by peak oxygen consumption (peak $\dot{V}o$). Ventilatory efficiency during exercise was represented by the $\dot{V}E$-$\dot{V}CO_2$ slope.[19]

Food Intake and Body Mass Analyses

Food intake for 3 consecutive days was assessed before ghrelin administration and during the last week of ghrelin therapy. Food intake was semiquantitatively assessed by a calorie count based on a 10-point scale method (0=null intake, 10=full intake or 1800 kcal), which was averaged for 3 days. Dual x-ray absorptiometry (DPX-L, Lunar Radiation) was repeated in all patients to examine changes in lean body mass, fat mass, and bone mineral content. Hand-grip strength was determined with a dynamometer.

Blood Sampling and Assay

Blood samples were taken from the antecubital vein the morning after an overnight fast. Serum GH and IGF-1 were measured by immunoradiometric assay (Ab Bead HGH Eiken, Eiken Chemical Co, Ltd, sensitivity=0.1 ng/mL; Somatomedin CII Bayer, Bayer Medical Ltd, sensitivity=0.3 ng/mL). Plasma norepinephrine and epinephrine were measured by high-performance liquid chromatography (HLC8030, Tosoh Co, sensitivity=6 pg/mL). Serum cortisol and insulin were measured by enzyme immunoassay (AIA-PACK CORT, sensitivity=0.2 μg/dL; AIA-PACK IRI, sensitivity=2.0 μU/mL, Tosoh Co). Serum tumor necrosis factor (TNF-α) and interleukin-6 (IL-6) were measured by enzyme immunoassay (Quantikine HS, R&D Systems Inc, sensitivity=0.18 pg/mL; TFB kit, TFB Co, Ltd, sensitivity=0.3 pg/mL). Plasma renin and aldosterone were measured with radioimmunoassay kits (RENIN RIABEAD, sensitivity=0.1 ng/mL; ALDOSTERONE RIAKIT II, sensitivity=2.0

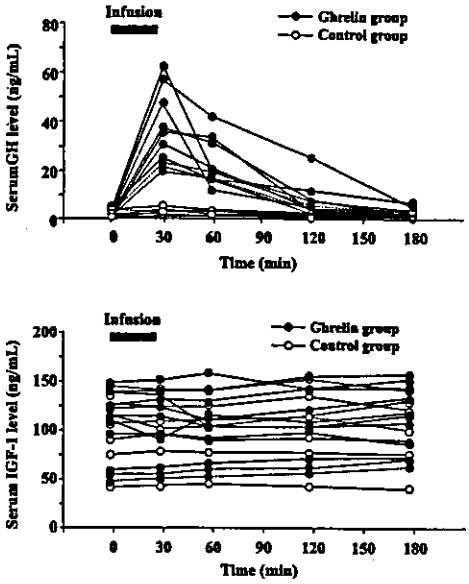

Figure 1. Changes in serum GH and IGF-1 after single administration of ghrelin. Solid line indicates cachectic patients; dotted line, noncachectic patients.

ng/dL, DAINABOT Co). Plasma brain natriuretic peptide (BNP) was measured by immunoradiometric assay (SHIONORIA BNP, sensitivity=4.0 pg/mL).

Statistical Analysis

Numerical values are expressed as mean±SEM. Comparisons of parameters between the 2 groups were made by unpaired Student's *t* test. Comparisons of the time course of serum GH and IGF-1 between the 2 groups were made by 2-way ANOVA for repeated measures, followed by the Newman-Keuls test. Comparisons of changes in parameters during the 3-week follow-up between the 2 groups were also made by 2-way ANOVA for repeated measures, followed by the Newman-Keuls test. A value of $P<0.05$ was considered significant.

Results

Administration of ghrelin transiently caused stomach rumbles in 6 patients and a slight feeling of being warm and sleepy in 4 subjects. Two patients felt slightly thirsty during ghrelin infusion. Other than these minor complaints, all subjects tolerated 3-week administration of ghrelin without incident. After 3-week administration of ghrelin, NYHA functional class improved in 4 patients and was unchanged in 6 patients. No change in NYHA functional class was observed in patients who did not receive ghrelin.

Effects of Ghrelin on Somatotropic Function

A single administration of ghrelin markedly increased serum GH level (baseline, 1.4±0.4; peak, 35.0±5.0 ng/mL; $P<0.001$; Figure 1). This elevation lasted >60 minutes after the start of ghrelin infusion. Serum IGF-1 level tended to increase 3 hours after the start of ghrelin infusion (101±12 to 110±12 ng/mL; $P=0.08$). Three-week administration of ghrelin tended to increase basal serum IGF-1 level (99±13 to 116±13 ng/mL; $P=0.07$). There was no significant difference in basal serum GH level between before and after 3 weeks of ghrelin therapy (2.0±0.8 to 1.2±0.3 ng/mL; P=NS).

Effects of Ghrelin on Food Intake, Body Weight, and Lean Body Mass

Administration of ghrelin significantly increased food intake (Figure 2). Three-week administration of ghrelin tended to increase body weight (49.6±2.7 to 50.4±2.7 kg; $P=0.09$). No development of edema was observed during ghrelin therapy. Dual x-ray absorptiometry demonstrated that treatment with ghrelin significantly increased lean body mass in patients with CHF (38.3±2.1 to 39.1±2.1 kg; $P<0.05$). Ghrelin did not significantly alter bone mineral content (2243±191 to 2265±189 g; P=NS) or fat mass (8877±1353 to 8748±1311 g; P=NS). Hand-grip strength was increased significantly by ghrelin therapy (20.5±1.7 to 22.7±2.0 kg; $P<0.01$). All of these parameters remained unchanged in patients who did not receive ghrelin.

Effects of Ghrelin on Cardiac Structure and Function

Neither heart rate nor blood pressure was significantly changed by 3-week administration of ghrelin (Table 2). Ghrelin increased LV ejection fraction (27±2% to 31±2%; $P<0.05$) in association with a decrease in LV end-systolic volume and an increase in LV mass (Figure 3), although ghrelin did not significantly alter LV end-diastolic volume. All of these parameters remained unchanged in patients who did not receive ghrelin.

Effects of Ghrelin on Exercise Capacity and Ventilatory Efficiency

Three-week administration of ghrelin significantly increased peak workload and peak $\dot{V}o$ during exercise (739±127 to 801±126 mL/min; $P<0.05$; Figure 4). Treatment with ghrelin did not significantly alter the $\dot{V}_E$–$\dot{V}co_2$ slope. In 1 patient

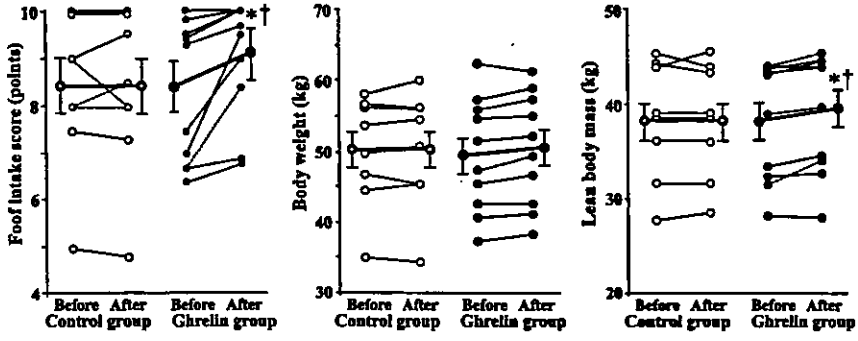

Figure 2. Food intake, body weight, and lean body mass before and after 3-week administration of ghrelin. Food intake was described semiquantitatively with 10-point scale method (0=null intake, 10=full intake). Data are mean±SEM. Solid line indicates cachectic patients; dotted line, noncachectic patients. *$P<0.05$ vs before; †$P<0.05$ vs respective control group.

TABLE 2. Physiological and Echocardiographic Measurements

	Control Group	Ghrelin Group
Heart rate, bpm		
Before	77±3	78±3
After	76±3	74±3
Mean arterial pressure, mm Hg		
Before	79±4	81±2
After	80±3	78±3
LVDd, mm		
Before	65.6±3.2	66.6±2.5
After	64.4±3.7	63.7±3.3
LVDs, mm		
Before	55.1±3.0	56.9 ± 2.9
After	53.9±3.6	52.8 ± 3.4*
FS, %		
Before	16.1±1.2	14.8±1.7
After	16.0±1.3	17.3±2.3
AWT diastole, mm		
Before	10.0±0.8	9.5±1.0
After	10.1±0.9	10.0±1.0*
PWT diastole, mm		
Before	9.2±0.4	9.3±0.6
After	9.4±0.4	9.9±0.5*†

LVDd indicates LV end-diastolic dimension; LVDs, LV end-systolic dimension; FS, fractional shortening; AWT, anterior wall thickness; and PWT, posterior wall thickness. Data are mean±SEM.

*$P<0.05$ vs before; †$P<0.05$ vs respective control group.

who did not undergo cardiopulmonary exercise testing, the distance walked in 6 minutes increased from 300 m to 410 m with ghrelin treatment. Exercise parameters remained unchanged without ghrelin.

Effects of Ghrelin on Sympathetic Nerve Activity

Three-week administration of ghrelin significantly decreased plasma norepinephrine and epinephrine (Figure 5). Treatment with ghrelin significantly decreased plasma BNP level (Table 3). Ghrelin did not significantly alter circulating glucose, insulin, cortisol, TNF-α, or IL-6. Neither plasma renin activity nor plasma aldosterone level was changed significantly. All of these parameters remained unchanged in patients who did not receive ghrelin.

Discussion

Ghrelin is a novel GH-releasing peptide that acts through a mechanism independent of that of hypothalamic GH-releasing hormone.[9] The GH-releasing effect of ghrelin has been shown to be more potent than that of GH-releasing hormone.[20] In fact, in the present study, ghrelin infusion elicited potent GH release in patients with CHF. Three-week administration of ghrelin increased LV ejection fraction in association with an increase in LV mass, which is consistent with findings from a previous experimental study in rats.[16] Plasma BNP level, a marker for LV function and wall stress, was decreased by ghrelin therapy. GH and its mediator, IGF-1, have been shown to enhance physiological compensatory hypertrophy in rats with CHF, resulting in a decrease in LV wall stress, leading to improvement in cardiac function.[21] Thus, ghrelin may also improve cardiac function partly through GH-dependent mechanisms. On the other hand, Baldanzi et al[22] have shown that ghrelin inhibits apoptosis of cardiomyocytes and endothelial cells through activation of extracellular signal-regulated kinase-1/2 and Akt serine kinases. Furthermore, stimulation of GHS-R by hexarelin has been shown to prevent cardiac damage after ischemia-reperfusion in hypophysectomized rats.[23] When these results are considered together, improvement in cardiac function by ghrelin therapy may be related to direct effects of ghrelin on myocardium. Importantly, ghrelin significantly decreased plasma norepinephrine levels in the present study. It is possible that improvement in cardiac function may lead to attenuation of sympathetic nerve activity. Interestingly, a recent study has demonstrated that ghrelin acts directly on the central nerve system to decrease sympathetic nerve activity.[24] Thus, inhibitory effects of ghrelin on sympathetic nerve activity may contribute to a decrease in plasma norepinephrine, which may have beneficial effects on cardiac performance in patients with CHF.

In the present study, 3-week administration of ghrelin improved exercise capacity in patients with CHF, as indicated by an increase in peak workload and peak $\dot{V}o$. A decrease in peak $\dot{V}o$ in patients with CHF is attributable not only to an inadequate increase in cardiac output during exercise, which is a central effect, but also to muscle wasting, a peripheral effect. Recently, we have shown that infusion of ghrelin increases cardiac output in patients with CHF.[12] In the present study, ghrelin increased lean body mass and muscle strength. These results suggest that ghrelin may improve exercise capacity through both central and peripheral effects.

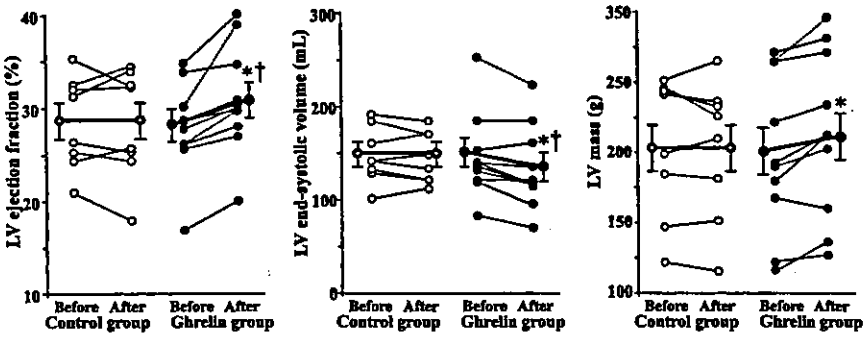

Figure 3. LV geometry and function before and after ghrelin therapy. Data are mean±SEM. Solid line indicates cachectic patients; dotted line, noncachectic patients. *$P<0.05$ vs before; †$P<0.05$ vs respective control group.

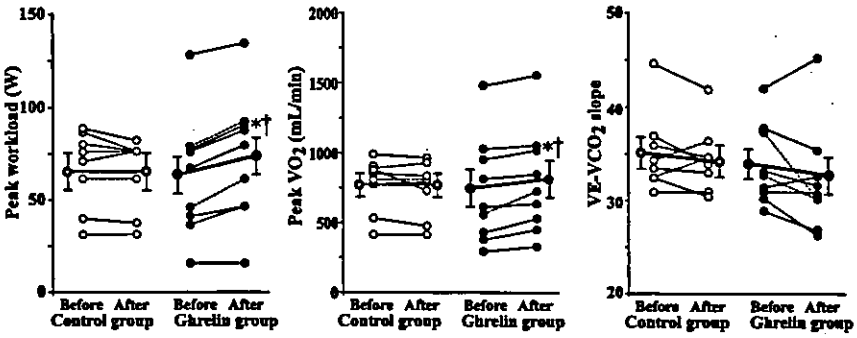

Figure 4. Exercise capacity and ventilatory efficiency before and after ghrelin therapy. Data are mean±SEM. Solid line indicates cachectic patients; dotted line, noncachectic patients. *$P<0.05$ vs before; †$P<0.05$ vs respective control group.

Cardiac cachexia, a catabolic state characterized by weight loss and muscle wasting, occurs frequently in patients with end-stage CHF[25] and is a strong independent risk factor for mortality in such patients.[26] Recently, we have shown that plasma ghrelin level is increased in cachectic patients with CHF as a compensatory mechanism in response to anabolic-catabolic imbalance.[17] In the present study, 3-week administration of ghrelin tended to increase body weight and significantly increased lean body mass and muscle strength. These results suggest that treatment with ghrelin improves muscle wasting in patients with CHF. These effects may be mediated, at least in part, by GH/IGF-1, which is considered essential for skeletal muscle. Earlier studies have shown that ghrelin induces orexigenic effects via activation of neuropeptide Y neurons in the hypothalamic arcuate nucleus.[13,14] In the present study, intravenous administration of ghrelin increased food intake in patients with CHF, which may contribute to anabolic effects of ghrelin. Tschop et al[15] have shown that administration of ghrelin induces adiposity through a GH-independent mechanism. In the present study, however, ghrelin did not significantly increase fat mass. This difference may be explained by the high dose of ghrelin (>2000-fold) used by Tschop et al. Ghrelin itself decreases fat utilization and increases fat, whereas GH decreases fat tissue and increases lean tissue. Thus, in the present study, ghrelin-induced GH may have attenuated an increase in fat and enhanced an increase in lean tissue.

The major limitation of this pilot trial relates to the lack of a randomized, placebo-controlled group. Patients in the control group were not treated identically because a placebo infusion was not performed. Nonetheless, this study was performed while patients were in a stable clinical condition during hospitalization. In addition, 8 patients in the control group were studied to exclude time-course effects during hospitalization. On the basis of the results of this study, a double-blind, randomized, and placebo-controlled study should be conducted. Second, this clinical study did not clarify mechanisms of increased LV ejection fraction by ghrelin therapy. Further studies are necessary to examine which mechanism predominantly contributes to improvement in LV ejection fraction.

Except for a few minor complications, long-term treatment with ghrelin was tolerated well in patients with CHF. Although a preliminary study documented the beneficial effects

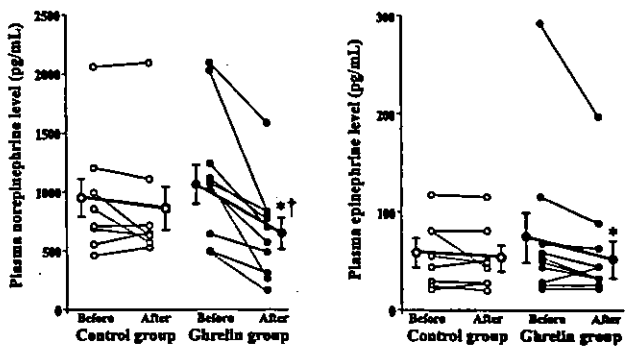

Figure 5. Plasma levels of norepinephrine and epinephrine before and after ghrelin therapy. Data are mean±SEM. Solid line indicates cachectic patients; dotted line, noncachectic patients. *$P<0.05$ vs before; †$P<0.05$ vs respective control group.

TABLE 3. Hormone Analysis in Patients With CHF

	Control Group	Ghrelin Group
BNP, pg/mL		
Before	180±53	238±59
After	181±62	190±60*
Fasting glucose, mg/dL		
Before	105±5	101±4
After	102±6	102±7
Insulin, μU/mL		
Before	6.0±1.4	3.9±0.7
After	6.8±2.0	5.5±1.2
Cortisol, μg/dL		
Before	15.5±1.9	17.9±1.6
After	14.5±2.6	17.2±1.5
TNF-α, pg/mL		
Before	5.3±0.9	5.7±0.8
After	5.4±0.9	5.6±0.8
IL-6, pg/mL		
Before	3.2±0.5	3.8±0.7
After	3.4±0.5	3.6±0.7
Renin, $ng \cdot mL^{-1} \cdot h^{-1}$		
Before	9.3±4.6	7.3±3.0
After	10.1±4.1	6.9±3.7
Aldosterone, ng/dL		
Before	11.6±4.1	15.0±4.7
After	12.7±4.1	11.9±4.2

Data are mean±SEM.
*$P<0.05$ vs before.

of GH,[5] controlled studies in humans have been predominantly negative.[7,8] Nevertheless, ghrelin has been shown to have GH-independent effects, stimulating vasodilation,[10–12] reversing cachexia,[13–15] and inhibiting sympathetic nerve activity[24] and myocyte apoptosis.[22] Thus, ghrelin may have additional therapeutic potential compared with GH supplementation. Ghrelin improved cardiac function and exercise capacity in not only cachectic CHF patients but also noncachectic ones. Nevertheless, the best candidates may be cachectic CHF patients because ghrelin stimulates feeding and improves muscle wasting.

Conclusions

These preliminary results suggest that repeated administration of ghrelin improves LV structure and function, exercise capacity, and muscle wasting in patients with CHF. Thus, administration of ghrelin may be a new therapeutic approach for the treatment of CHF.

Acknowledgments

This work was supported by Research Grant for Cardiovascular Disease 16C-6 from the Ministry of Health, Labor and Welfare; Industrial Technology Research Grant Program in 2003 from the New Energy and Industrial Technology Development Organization of Japan; Health and Labor Sciences Research Grants–Genome 005, Mochida Memorial Foundation for Medical and Pharmaceutical Research; and the Promotion of Fundamental Studies in Health Science of the Organization for Pharmaceutical Safety and Research of Japan.

References

1. Dec GW, Fuster V. Idiopathic dilated cardiomyopathy. *N Engl J Med.* 1994;331:1564–1575.
2. Pittman JG, Cohen P. The pathogenesis of cardiac cachexia. *N Engl J Med.* 1964;271:403–409.
3. Amato G, Carella C, Fazio S, et al. Body composition, bone metabolism, heart structure and function in growth hormone deficient adults before and after growth hormone replacement therapy at low doses. *J Clin Endocrinol Metab.* 1993;77:1671–1676.
4. Fuller J, Mynett JR, Sugden PH. Stimulation of cardiac protein synthesis by insulin-like growth factors. *Biochem J.* 1992;282:85–90.
5. Fazio S, Sabatini D, Capaldo B, et al. A preliminary study of growth hormone in the treatment of dilated cardiomyopathy. *N Engl J Med.* 1996;334:809–814.
6. Anker SD, Volterrani M, Pflaum CD, et al. Acquired growth hormone resistance in patients with chronic heart failure: implications for therapy with growth hormone. *J Am Coll Cardiol.* 2001;38:443–452.
7. Osterziel KJ, Strohm O, Schuler J, et al. Randomised, double-blind, placebo-controlled trial of human recombinant growth hormone in patients with chronic heart failure due to dilated cardiomyopathy. *Lancet.* 1998;351:1233–1237.
8. Isgaard J, Bergh CH, Caidahl K, et al. A placebo-controlled study of growth hormone in patients with congestive heart failure. *Eur Heart J.* 1998;19:1704–1711.
9. Kojima M, Hosoda H, Date Y, et al. Ghrelin is a growth-hormone-releasing acylated peptide from stomach. *Nature.* 1999;402:656–660.
10. Nagaya N, Kojima M, Uematsu M, et al. Hemodynamic and hormonal effects of human ghrelin in healthy volunteers. *Am J Physiol Regul Integr Comp Physiol.* 2001;280:R1483–R1487.
11. Wiley KE, Davenport AP. Comparison of vasodilators in human internal mammary artery: ghrelin is a potent physiological antagonist of endothelin-1. *Br J Pharmacol.* 2002;136:1146–1152.
12. Nagaya N, Miyatake K, Uematsu M, et al. Hemodynamic, renal and hormonal effects of ghrelin infusion in patients with chronic heart failure. *J Clin Endocrinol Metab.* 2001;86:5854–5859.
13. Nakazato M, Murakami N, Date Y, et al. A role for ghrelin in the central regulation of feeding. *Nature.* 2001;409:194–198.
14. Shintani M, Ogawa Y, Ebihara K, et al. Ghrelin, an endogenous growth hormone secretagogue, is a novel orexigenic peptide that antagonizes leptin action through the activation of hypothalamic neuropeptide Y/Y1 receptor pathway. *Diabetes.* 2001;50:227–232.
15. Tschop M, Smiley DL, Heiman ML. Ghrelin induces adiposity in rodents. *Nature.* 2000;407:908–913.
16. Nagaya N, Uematsu M, Kojima M, et al. Chronic administration of ghrelin improves left ventricular dysfunction and attenuates development of cardiac cachexia in rats with heart failure. *Circulation.* 2001;104:1430–1435.
17. Nagaya N, Uematsu M, Kojima M, et al. Elevated circulating levels of ghrelin in the cachexia associated with chronic heart failure. *Circulation.* 2001;104:2034–2038.
18. Schiller NB, Acquatella H, Ports TA, et al. Left ventricular volume from paired biplane two-dimensional echocardiography. *Circulation.* 1979;60:547–555.
19. Nagaya N, Uematsu M, Oya H, et al. Short-term oral administration of L-arginine improves hemodynamics and exercise capacity in patients with precapillary pulmonary hypertension. *Am J Respir Crit Care Med.* 2001;163:887–891.
20. Takaya K, Ariyasu H, Kanamoto N, et al. Ghrelin strongly stimulates growth hormone (GH) release in humans. *J Clin Endocrinol Metab.* 2000;85:4908–4911.
21. Cittadini A, Grossman JD, Napoli R, et al. Growth hormone attenuates early left ventricular remodeling and improves cardiac function in rats with large myocardial infarction. *J Am Coll Cardiol.* 1997;29:1109–1116.
22. Baldanzi G, Filigheddu N, Cutrupi S, et al. Ghrelin and des-acyl ghrelin inhibit cell death in cardiomyocytes and endothelial cells through ERK1/2 and PI 3-kinase/AKT. *J Cell Biol.* 2002;159:1029–1037.
23. Locatelli V, Rossoni G, Schweiger F, et al. Growth hormone–independent cardioprotective effects of hexarelin in the rat. *Endocrinology.* 1999;140:4024–4031.
24. Matsumura K, Tsuchihashi T, Fujii K, et al. Central ghrelin modulates sympathetic activity in conscious rabbits. *Hypertension.* 2002;40:694–699.
25. Anker SD, Negassa A, Coats AJ, et al. Prognostic importance of weight loss in chronic heart failure and the effect of treatment with angiotensin-converting-enzyme inhibitors: an observational study. *Lancet.* 2003;361:1077–1083.
26. Anker SD, Ponikowski P, Varney S, et al. Wasting as independent risk factor for mortality in chronic heart failure. *Lancet.* 1997;349:1050–1053.

Adrenomedullin Enhances Angiogenic Potency of Bone Marrow Transplantation in a Rat Model of Hindlimb Ischemia

Takashi Iwase, MD; Noritoshi Nagaya, MD; Takafumi Fujii, MD; Takefumi Itoh, MD; Hatsue Ishibashi-Ueda, MD; Masakazu Yamagishi, MD; Kunio Miyatake, MD; Toshio Matsumoto, MD; Soichiro Kitamura, MD; Kenji Kangawa, PhD

Background—Previous studies have shown that adrenomedullin (AM) inhibits vascular endothelial cell apoptosis and induces angiogenesis. We investigated whether AM enhances bone marrow cell–induced angiogenesis.

Methods and Results—Immediately after hindlimb ischemia was created, rats were randomized to receive AM infusion plus bone marrow–derived mononuclear cell (MNC) transplantation (AM+MNC group), AM infusion alone (AM group), MNC transplantation alone (MNC group), or vehicle infusion (control group). The laser Doppler perfusion index was significantly higher in the AM and MNC groups than in the control group (0.74±0.11 and 0.69±0.07 versus 0.59±0.07, respectively, $P<0.01$), which suggests the angiogenic potency of AM and MNC. Importantly, improvement in blood perfusion was marked in the AM+MNC group (0.84±0.08). Capillary density was highest in the AM+MNC group, followed by the AM and MNC groups. In vitro, AM inhibited MNC apoptosis, promoted MNC adhesiveness to a human umbilical vein endothelial cell monolayer, and increased the number of MNC-derived endothelial progenitor cells. In vivo, AM administration not only enhanced the differentiation of MNC into endothelial cells but also produced mature vessels that included smooth muscle cells.

Conclusions—A combination of AM infusion and MNC transplantation caused significantly greater improvement in hindlimb ischemia than MNC transplantation alone. This effect may be mediated in part by the angiogenic potency of AM itself and the beneficial effects of AM on the survival, adhesion, and differentiation of transplanted MNCs. (***Circulation.*** **2005;111:356-362.)**

Key Words: peptides ■ angiogenesis ■ peripheral vascular disease

Peripheral vascular disease is a crucial health issue that affects an estimated 27 million people.[1] Despite recent advances in medical intervention, the symptoms of some patients with critical limb ischemia fail to be controlled. Bone marrow–derived mononuclear cells (MNCs) include a variety of stem and progenitor cells, such as endothelial progenitor cells (EPCs), and contribute to pathological neovascularization.[2] MNC transplantation induces therapeutic angiogenesis in ischemic limb[3,4]; however, some patients fail to respond to this cell therapy. Thus, a novel therapeutic strategy to enhance the angiogenic property of MNCs is desirable.

Adrenomedullin (AM) is a potent vasodilator peptide that was originally isolated from human pheochromocytoma.[5] Previous studies have reported that abnormalities of vascular structure are present in homozygous AM knockout mice.[6,7] A recent study has demonstrated that blood flow recovery in ischemic limb and tumor angiogenesis are substantially impaired in heterozygous AM knockout mice.[8] Furthermore, AM has been shown to inhibit vascular endothelial cell apoptosis and induce angiogenesis through the activation of the phosphatidylinositol 3-kinase (PI3K)/Akt pathway.[9,10] These results suggest that AM is indispensable for modulating angiogenesis and vasculogenesis. When these findings are taken together, combination therapy with MNC transplantation and AM infusion may have additional or synergetic effects on therapeutic angiogenesis for the treatment of severe peripheral vascular disease. Thus, the purposes of the present study were (1) to investigate whether local infusion of AM enhances the angiogenic potency of MNC transplantation in a rat model of hindlimb ischemia and (2) to investigate the effects of AM on the survival, adhesion, and differentiation of transplanted MNCs.

Received June 18, 2004; revision received September 9, 2004; accepted November 3, 2004.

From the Departments of Regenerative Medicine and Tissue Engineering (T. Iwase, N.N., T. Itoh), Cardiac Physiology (T.F.), and Biochemistry (K.K.), National Cardiovascular Center Research Institute, Osaka, Japan; Departments of Internal Medicine (N.N., M.Y., K.M.), Pathology (H.I.-U.), and Cardiovascular Surgery (S.K.), National Cardiovascular Center, Osaka, Japan; and Department of Medicine and Bioregulatory Sciences (T. Iwase, T.M.), University of Tokushima Graduate School of Medicine, Tokushima, Japan.

Reprint requests to Noritoshi Nagaya, MD, Department of Regenerative Medicine and Tissue Engineering, National Cardiovascular Center Research Institute, 5-7-1 Fujishirodai, Suita, Osaka 565-8565, Japan. E-mail nagayann@hsp.ncvc.go.jp

Circulation is available at http://www.circulationaha.org

DOI: 10.1161/01.CIR.0000153352.29335.B9

Methods

Animal Model of Hindlimb Ischemia

Male Lewis rats (weight 250 to 275 g; Japan SLC Inc, Hamamatsu, Japan) were used in the present study. The left common iliac artery of each rat was resected under anesthesia with pentobarbital sodium (50 mg/kg). The distal portion of the saphenous artery and all side branches and veins were dissected free and excised. The right hindlimb was kept intact and used as the nonischemic limb. Transplantation of bone marrow–derived MNCs and infusion of AM were performed in 40 rats immediately after hindlimb ischemia was created. This protocol resulted in the creation of 4 groups: (1) AM infusion plus MNC transplantation (AM+MNC group, n=10), (2) AM infusion plus PBS injection (AM group, n=10), (3) vehicle infusion plus MNC transplantation (MNC group, n=10), and (4) vehicle infusion plus PBS injection (control group, n=10). The Animal Care Committee of the National Cardiovascular Center approved this experimental protocol.

MNC Transplantation and AM Infusion

Bone marrow was harvested from the femur and tibia in other male Lewis rats, and MNCs were isolated by Ficoll density gradient centrifugation (Lymphoprep, Nycomed). MNCs (5×10^6 cells per animal) or PBS was injected into the ischemic thigh muscle with a 26-gauge needle at 5 different points. Human recombinant AM (0.01 $\mu g \cdot kg^{-1} \cdot min^{-1}$) or vehicle was administered for 7 days with a mini-osmotic pump (ALZET, Palo Alto) implanted in the left inguinal region.

Assessment of Blood Perfusion

To measure serial blood flow for 3 weeks, we used a laser Doppler perfusion image (LDPI) analyzer (Moor Instrument). After blood flow was scanned twice, the average flow values of the ischemic and nonischemic limbs were calculated by computer-assisted quantification. The LDPI index was determined as the ratio of ischemic to nonischemic hindlimb blood perfusion.[11]

Histological Assessment

Three weeks after MNC transplantation and/or AM infusion, 4 pieces of ischemic tissue from the adductor and semimembranous muscles were obtained and snap-frozen in liquid nitrogen. Frozen tissue sections were stained with alkaline phosphatase by an indoxyl tetrazolium method to detect capillary endothelial cells.[3,11] Five fields were randomly selected to count the number of capillaries. The capillary number adjusted per muscle fiber was used to compare the differences in capillary density among the 4 groups.[3]

Monitoring of Transplanted MNCs in Ischemic Hindlimb Muscle

To examine differentiation of transplanted MNCs, 5×10^6 MNCs labeled with red fluorescent dye (PKH26-GL, Sigma Chemical Co) were transplanted into the ischemic thigh muscle in rats with (n=3) and without (n=3) AM infusion. Three weeks after transplantation, frozen tissue sections from ischemic muscle were incubated with anti-von Willebrand factor antibody (vWF, DAKO), anti-CD31 antibody (BD Pharmingen), and anti-α-smooth muscle actin antibody (α-SMA, DAKO), followed by incubation with Alexa Fluor 633 IgG antibody (Molecular Probes) and FITC-conjugated IgG antibody (BD Pharmingen), respectively. Five high-power fields (40×) of each section were randomly selected to count the number of transplanted MNCs, vWF-positive cells, and α-SMA–positive cells.

In Situ Detection of MNC Apoptosis

PKH26-labeled MNCs (5×10^6 cells per animal) were transplanted into the ischemic muscle in rats with (n=2) and without (n=2) AM infusion. Twenty-four hours after transplantation, apoptosis of transplanted MNCs in ischemic tissue was evaluated by terminal dUTP nick-end labeling (TUNEL) assay (ApopTag Fluorescein kit, Serological Corporation), as reported previously.[12]

In Vitro Apoptosis Assay

The antiapoptotic effect of AM on MNCs was evaluated by TUNEL assay. Human MNCs, isolated from peripheral blood, were plated on 12-well plates (1×10^6 cells per well) and cultured in serum-free medium for 24 hours with control buffer, AM, or AM plus wortmannin, a PI3K inhibitor (50 nmol/L). TUNEL for detection of apoptotic nuclei was performed according to the manufacturer's instructions. MNCs were then mounted in medium that contained 4′,6-diamidino-2-phenylindole (DAPI). Randomly selected microscopic fields (n=10) were evaluated to calculate the ratio of TUNEL-positive cells to total cells.

Adhesion Assay

We evaluated whether AM enhances MNC adhesiveness according to a previously reported method.[13] In brief, human umbilical vein endothelial cells (HUVECs) were cultured to confluence on 6-well plates with or without pretreatment with tumor necrosis factor-α (1 ng/mL). In the absence or presence of AM (10^{-7} mol/L), 1×10^6 MNCs labeled with PKH26 were incubated on an HUVEC monolayer for 24 hours. Nonadherent MNCs were removed, and the number of PKH26-positive cells in each well was counted.

Cell ELISA

Expression of adhesion molecules in HUVECs was measured by cell ELISA, as reported previously.[14] In brief, confluent HUVECs on 96-well plates were treated with AM (10^{-7} mol/L) or control buffer for 4 hours. HUVECs were then incubated with monoclonal mouse antibodies against intercellular adhesion molecule-1 (ICAM-1, R&D Systems) and vascular adhesion molecule-1 (VCAM-1, R&D Systems). A protein detector ELISA kit (KPL) was used to detect bound monoclonal antibodies.

EPC Culture Assay

Culture of EPCs was performed as described previously.[11,15,16] In brief, 2×10^6 MNCs were plated in Medium-199 supplemented with 20% FCS, heparin, and antibiotics on fibronectin-coated 6-well plates. AM (10^{-7} mol/L), human recombinant vascular endothelial growth factor (VEGF; 20 ng/mL), or control buffer was added to each plate. After 7 days of culture, nonadherent cells were removed, and adherent cells were incubated with acetylated LDL labeled with DiI (DiI-acLDL, Biomedical Technologies) and FITC-labeled lectin from ulex europaeus (Sigma). Double-positive cells for DiI-acLDL and FITC-labeled lectin were identified as EPCs.[16] Randomly selected microscopic fields (n=10) were evaluated to count the number of EPCs.

Fluorescence-Activated Cell Sorting Analysis

Fluorescence-activated cell sorting was performed to identify characteristics of adherent cells after 7 days of culture.[16] Cells were incubated for 30 minutes at 4°C with anti-human CD31 antibodies (clone L133.1, Becton Dickinson), anti-human KDR antibodies (clone KDR-1, Sigma), and anti-human VE-cadherin antibodies (clone BV6, Chemicon). Isotype-identical antibodies served as controls. Fluorescence-activated cell sorting analyses were performed with a FACSCalibur flow cytometer and Cell Quest software (BD Biosciences).

Real-Time Polymerase Chain Reaction

Expression of calcitonin receptor-like receptor (CRLR), a receptor for AM, was examined by real-time polymerase chain reaction (PCR). Total RNA was extracted from MNCs, EPCs, and HUVECs with an RNA extraction kit (RNeasy Mini Kit, Qiagen) and converted to cDNA by reverse transcription. Real-time PCR was performed with SYBR green dye (QuantiTect SYBR Green PCR kit, Qiagen) and a Prism 7700 sequence detection system (Applied Biosystems). The PCR primers for CRLR were as follows: sense primer 5′-CATTCAACAAGCAGAAGGCG-3′ and antisense primer 5′-AGCCATCCATCCCAGGTTC-3′. For GAPDH, the primers were as follows: sense primer 5′-CAATGCCTCCTGCACCACCAA-3′ and antisense primer 5′-GAGGCAGGGATGATGTTCTGGA-3′. Levels of CRLR mRNA were normalized to that of

GAPDH mRNA. PCR-amplified products were also electrophoresed on 2% agarose gels to confirm that single bands were amplified.

In Vitro Matrigel Assay

HUVECs (1×10^5 cells) were seeded onto 24-well plates coated with Matrigel (Becton Dickinson) in the presence of the combination of control buffer, AM (10^{-7} mol/L), VEGF (10 ng/mL), or neutralizing antibodies against KDR (2 μg/mL, R&D Systems). After incubation for 18 hours, tube formation area was measured as described previously.[17] The control was defined as 100% tube formation, and the percent increase was calculated for each sample.

Measurements of Cytokines

A total of 1×10^6 MNCs or HUVECs were plated in serum-free medium with or without AM (10^{-7} mol/L) on 12-well plates. After 24-hour incubation, the conditioned medium was collected, and VEGF, basic fibroblast growth factor, and hepatocyte growth factor were measured with enzyme immunoassay kits (R&D Systems).

Migration Assay

Migration assay of smooth muscle cells (SMCs) was performed with Transwell (Coster) 24-well plates composed of a collagen-coated membrane with 8-μm pores. Human aortic SMCs, preincubated with serum-free medium for 24 hours to maintain quiescence, were seeded on the upper chamber at a concentration of 1×10^6 cells/mL. Serum-free medium containing control buffer, AM (10^{-7} mol/L), or AM plus wortmannin (50 nmol/L) was placed in the lower chamber. After incubation for 12 hours, the number of migrated cells was counted in the randomly selected fields (n=5).

Statistical Analysis

All values are expressed as mean±SEM. Student's unpaired *t* test was used to compare differences between 2 groups. Comparisons of parameters among 3 or 4 groups were made by 1-way ANOVA, followed by Scheffé multiple comparison test. Comparisons of the time course of the LDPI index were made by 2-way ANOVA for repeated measures, followed by Scheffé multiple comparison tests. A probability value <0.05 was considered statistically significant.

Results

Blood Perfusion and Capillary Density

Blood perfusion of the ischemic hindlimb increased modestly but gradually in the AM and MNC groups after treatment (Figure 1A). Interestingly, blood perfusion in the AM+MNC group markedly improved within 2 weeks after treatment and showed further improvement thereafter. The LDPI index was significantly higher in the AM, MNC, and AM+MNC groups than in the control group 3 weeks after surgery (Figure 1B). Importantly, the LDPI index was highest in the AM+MNC group among the 4 groups.

Alkaline phosphatase staining of ischemic muscle showed significant augmentation of neovascularization in the AM, MNC, and AM+MNC groups (Figure 2A). The capillary/muscle fiber ratio of ischemic muscle was highest in the AM+MNC group, followed by the MNC group, AM group, and control group (Figure 2B).

Differentiation of Transplanted MNCs

Three weeks after MNC transplantation, PKH26-labeled MNCs were frequently observed in the AM+MNC group, and these transplanted cells were positive for vWF (Figure 3A). Most of these cells were also stained by CD31 (data not shown). The number of PKH26/vWF double-positive cells was significantly higher in the AM+MNC group than in the

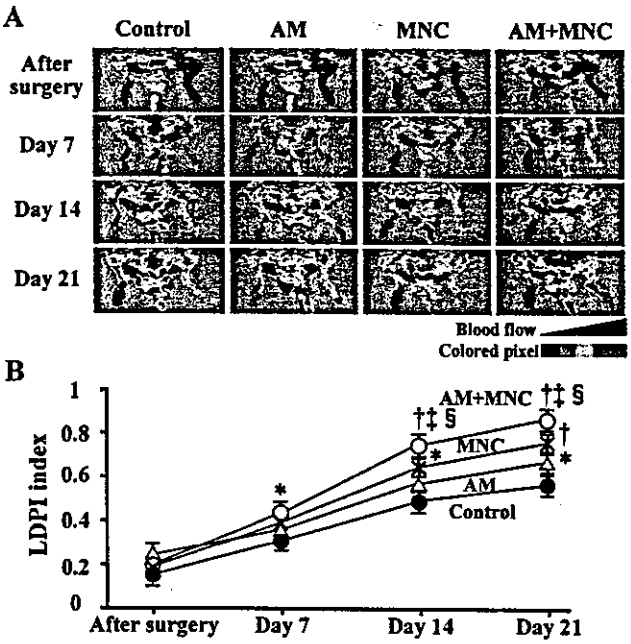

Figure 1. A, Representative examples of serial laser Doppler perfusion images. Blood perfusion of ischemic hindlimb increased notably in AM+MNC group (red to yellow). B, Quantitative analysis of hindlimb blood perfusion with LDPI index, ratio of ischemic to nonischemic hindlimb blood perfusion. Data are mean±SEM. *$P<0.05$ and †$P<0.01$ vs control; ‡$P<0.01$ vs AM; §$P<0.05$ vs MNC.

MNC group (Figure 3B). Although PKH26/α-SMA double-positive cells were not detected in ischemic muscle of each group, newly formed vascular structures in the AM+MNC group included α-SMA–positive cells (Figure 3C). The number of α-SMA–positive cells in the MNC-derived vascular structures was significantly higher in the AM+MNC group than in the MNC group (Figure 3D).

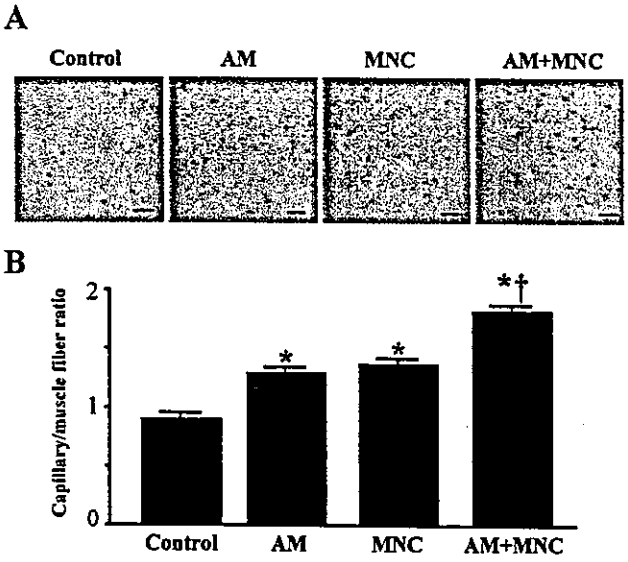

Figure 2. A, Representative photographs of alkaline phosphatase staining in ischemic hindlimb muscles. Capillary density in AM+MNC group was markedly higher than that in other groups. B, Quantitative analysis of capillary density in ischemic hindlimb muscles. Data are mean±SEM. *$P<0.01$ vs control; †$P<0.01$ vs AM and MNC. Scale bars: 50 μm.

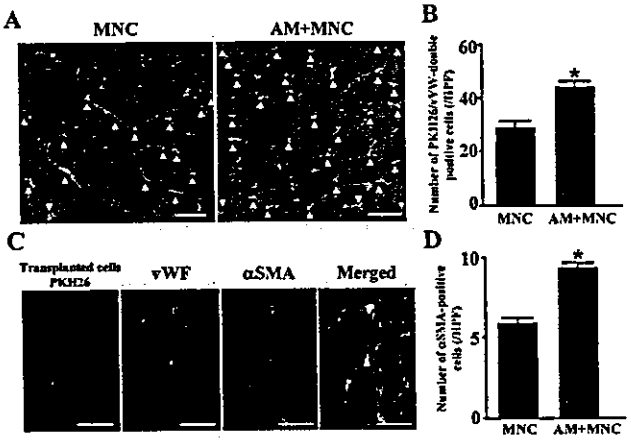

Figure 3. In vivo differentiation of transplanted MNCs. A, Representative photographs of MNC-derived vascular structures in MNC and AM+MNC groups. Red fluorescence (PKH26)–labeled MNCs were transplanted into ischemic thigh muscle. PKH26 (red)/vWF (blue) double-positive cells (pink, arrows) were frequently observed in AM+MNC group. B, Number of PKH26/vWF double-positive cells (MNC-derived endothelial cells) was significantly higher in AM+MNC group than in MNC group. C, Representative photographs of newly formed mature vessels in AM+MNC group. MNC-derived vascular structures often included α-SMA–positive cells (green). D, Number of α-SMA–positive cells in MNC-derived vessels was significantly higher in AM+MNC group than in MNC group. Data are mean±SEM. *$P<0.01$ vs MNC. Bars: 50 μm. HPF indicates high-power field.

Antiapoptotic Effect of AM on MNCs

In vitro, serum starvation induced MNC apoptosis, as indicated by detection of TUNEL-positive cells (Figure 4A). When incubated in the presence of AM, the percentage of TUNEL-positive cells markedly decreased in a dose-dependent manner (Figure 4B). However, pretreatment with wortmannin, a PI3K inhibitor, diminished the antiapoptotic effect of AM. Similarly, in vivo, local administration of AM decreased TUNEL-positive MNC 24 hours after transplantation (data not shown).

Effect of AM on MNC Adhesiveness

The number of adherent MNCs on an HUVEC monolayer increased significantly in the presence of AM (10^{-7} mol/L) compared with control (Figures 5A and 5B). With pretreatment using tumor necrosis factor-α, AM also enhanced the adhesiveness of MNCs to HUVECs. AM significantly enhanced expression of ICAM-1 and VCAM-1 in HUVECs (Figure 5C).

Effect of AM on EPC Expansion

After 7-day culture of human MNCs, spindle-shaped or cobblestone-like adherent cells were observed (Figure 6A). Most of the adherent cells were double stained with DiI-acLDL and FITC-labeled lectin. These adherent cells expressed endothelial cell–specific markers: KDR, VE cadherin, and CD31 (Figure 6B). Thus, we identified the major population of the adherent cells as EPCs. Culture of MNCs with AM significantly increased the number of EPCs (Figure 6C). The effect of AM was equivalent to that of VEGF. Real-time PCR revealed that MNCs, EPCs, and HUVECs expressed mRNA of CRLR (Figure 6D). Expression of

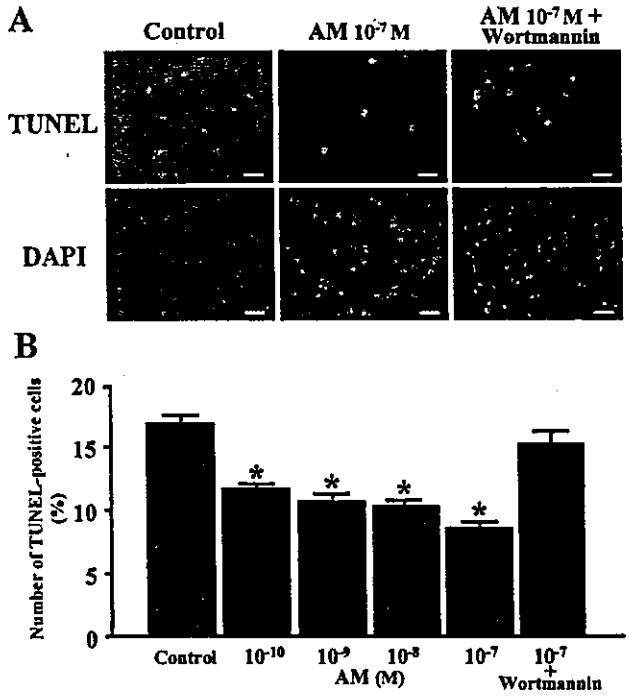

Figure 4. Apoptosis assay. A, Apoptosis of MNC was detected by TUNEL assay (green). Nuclei of MNC were stained with DAPI (blue). AM inhibited MNC apoptosis in serum-free medium. B, Quantitative analysis. AM decreased percentage of TUNEL-positive cells in dose-dependent manner. Pretreatment with wortmannin, a PI3K inhibitor, diminished antiapoptotic effect of AM. Data are mean±SEM. *$P<0.01$ vs control. Bars: 50 μm.

CRLR mRNA was highest in HUVECs, followed by EPCs and MNCs.

Effects of AM on Tube Formation and SMC Migration

Like VEGF, AM induced tube formation in HUVECs in vitro (Figure 7A). Blocking antibodies against KDR significantly inhibited VEGF-induced tube formation, whereas they did not suppress AM-induced tube formation (Figure 7B). AM did not significantly alter VEGF, basic fibroblast growth factor, or hepatocyte growth factor levels in conditioned medium of cultured MNCs or HUVECs (data not shown). AM significantly increased the number of migrated SMCs compared with control (Figures 7C and 7D). Pretreatment with wortmannin diminished the effect of AM on SMC migration.

Discussion

In the present study, we demonstrated in vivo that AM infusion or MNC transplantation alone induced angiogenesis in a rat model of hindlimb ischemia, the combination of AM infusion and MNC transplantation enhanced MNC-induced angiogenesis, and AM increased the number of MNC-derived vWF-positive cells and generated α-SMA–positive vascular structures. We also demonstrated in vitro that AM inhibited serum starvation–induced MNC apoptosis, promoted MNC adhesiveness to an HUVEC monolayer, increased the number of MNC-derived EPCs, and stimulated SMC migration.

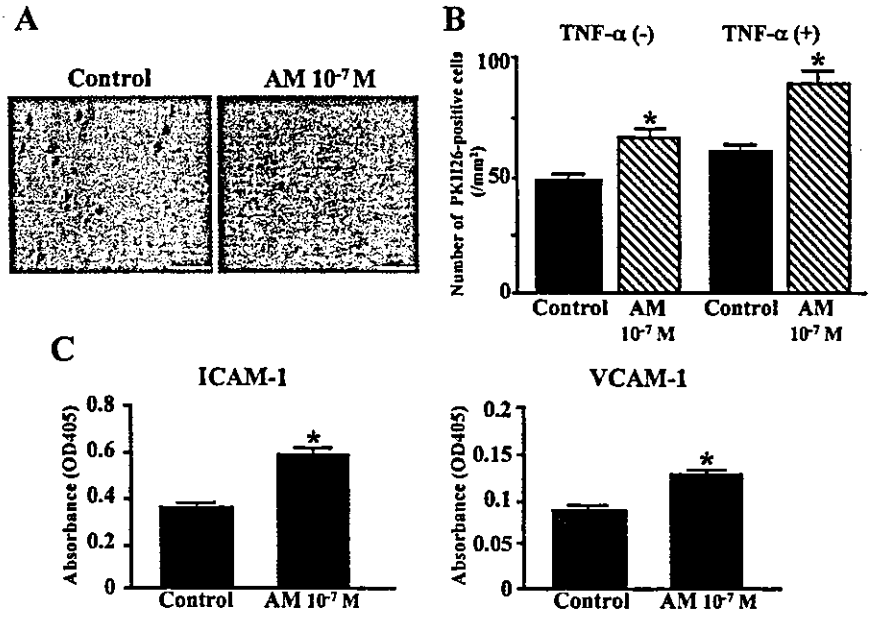

Figure 5. A and B, Adhesion assay. Representative photographs of red fluorescence–labeled MNC adhesion to HUVEC monolayer with and without AM (A). Quantitative analysis of MNC adhesion (B). Bars: 50 μm. C, Surface expression of ICAM-1 and VCAM-1 in HUVECs with or without AM. Data are mean±SEM. TNF indicates tumor necrosis factor. *P<0.01 vs control.

MNC transplantation causes therapeutic angiogenesis by supplying EPCs and multiple angiogenic cytokines such as VEGF.[3,4] The present study showed that local infusion of AM significantly increased blood perfusion and capillary density in ischemic hindlimb muscle. Furthermore, a combination of AM infusion and MNC transplantation significantly increased blood perfusion and capillary density of the ischemic hindlimb compared with MNC transplantation alone. AM has been shown to induce angiogenesis in vitro and in vivo through the PI3K/Akt pathway.[10,18] In the present study, AM-induced tube formation was not blocked by neutralizing antibodies against KDR. In addition, AM did not enhance VEGF secretion from MNCs and HUVECs. Thus, beneficial effects of combination therapy

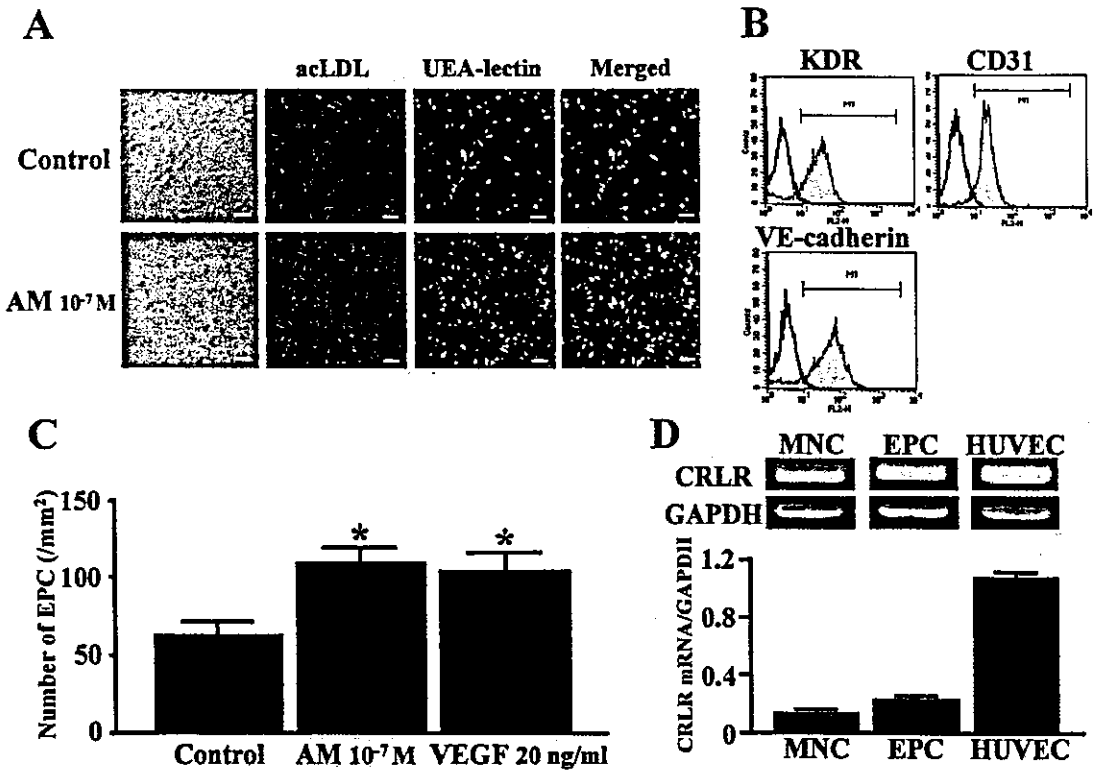

Figure 6. A through C, EPC culture assay. Cultured adherent cells took up DiI-acLDL (red) and FITC-labeled lectin (green) in same fields (A). Fluorescence-activated cell sorting analyses revealed that most adherent cells expressed KDR, VE cadherin, and CD31 (B). Culture of MNCs with AM significantly increased number of EPCs. Effect of AM was equivalent to that of VEGF (C). Data are mean±SEM. *P<0.01 vs control. Bars: 50 μm. D, Quantitative analysis of AM receptor (CRLR) mRNA expression in MNCs, EPCs, and HUVECs. UEA indicates ulex europaeus.

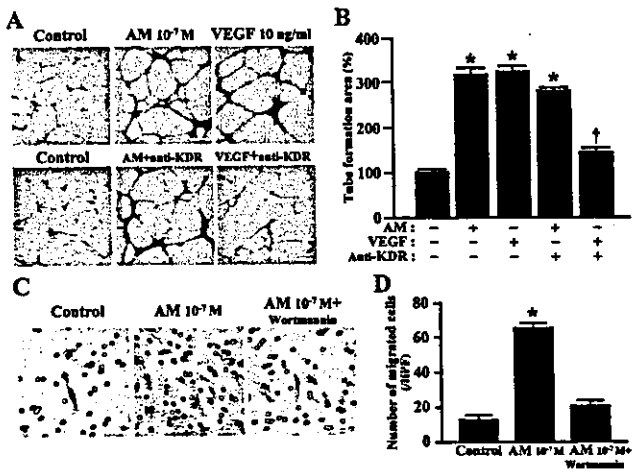

Figure 7. A and B, Matrigel assay. Representative photographs of tube formation (A). Quantitative analysis of tube formation area (B). Data are mean±SEM. *P<0.01 vs control; †P<0.01 vs VEGF. Bars: 20 μm. C and D, Migration assay. Representative photographs of migrated SMCs (C). Quantitative analyses of SMC migration (D). Data are mean±SEM. *P<0.01 vs control. Bars: 50 μm.

with AM and MNCs may be attributable in part to the angiogenic properties of AM itself.

An earlier study has shown that transplanted MNCs disappear from ischemic muscle 7 days after transplantation.[19] We demonstrated that apoptosis of MNCs occurred in ischemic muscle 24 hours after MNC transplantation. These results raise the possibility that the angiogenic potency of MNC transplantation is attenuated by MNC apoptosis. In the present study, AM inhibited apoptosis of MNCs in vitro and in vivo, and the antiapoptotic effect of AM was suppressed by wortmannin, a PI3K inhibitor. These findings suggest that AM prolongs MNC survival through the PI3K/Akt pathway and thereby enhances neovascularization in ischemic tissue.

In the present study, AM promoted adhesiveness of MNCs to an HUVEC monolayer. AM significantly enhanced expression of ICAM-1 and VCAM-1 in HUVECs, both of which facilitate adhesion of MNCs to endothelial cells.[20] These findings suggest that AM increases MNC adhesiveness to endothelial cells via activation of adhesion molecules. A recent study has shown that MNC adhesiveness to endothelial cells is indispensable for MNC differentiation into endothelial lineage.[21] Thus, it is possible that AM infusion enhances the angiogenic potency of MNCs at least in part through promotion of adhesion of MNC to host vascular endothelial cells.

VEGF has been shown to increase the number of EPCs in vitro and in vivo, resulting in angiogenesis and vasculogenesis.[13,22] The present study showed that MNCs and EPCs expressed CRLR, a receptor of AM. In vitro, AM increased the number of MNC-derived EPCs that expressed VE cadherin, KDR, and CD31. The effect of AM on EPC expansion was equivalent to that of VEGF. In vivo, AM infusion increased the number of MNC-derived vWF-positive cells, although incorporation of these cells in the capillaries may be due in part to incorporation of hematopoietic cells. These findings suggest that AM may accelerate MNC differentiation into endothelial lineage.

SMC is essential for the generation of functional and mature blood vessels.[23] We demonstrated in vivo that local infusion of AM increased the number of α-SMA–positive cells (SMCs) in MNC-derived vascular structures. In vitro, AM enhanced SMC migration, which was inhibited by wortmannin, a PI3K inhibitor. Recent studies using homozygous AM knockout mice have suggested that AM is indispensable for vascular morphogenesis.[6,7] When these findings are taken together, it is possible that AM contributes to vessel maturation through enhancement of SMC migration via the PI3K/Akt-dependent pathway.

Currently, a new therapeutic approach to augment the efficacy of MNC transplantation is awaited for the treatment of severe peripheral vascular disease. The present study demonstrated that local infusion of AM enhanced the angiogenic potency of MNC transplantation. In the present study, AM inhibited MNC apoptosis and increased the total number of engrafted cells in ischemic tissue, although this study did not show the effect of AM on specific cell populations of MNCs. In addition, AM promoted cell proliferation, migration, and differentiation. We have already demonstrated the safety of AM infusion in patients with congestive heart failure.[24] Thus, combination therapy with AM infusion and MNC transplantation may be a novel and promising therapeutic strategy for the treatment of severe peripheral vascular disease.

Conclusions

A combination of AM infusion and MNC transplantation caused significantly greater improvement in hindlimb ischemia than MNC transplantation alone. This effect may be mediated in part by the angiogenic potency of AM itself and the beneficial effects of AM on the survival, adhesion, and differentiation of transplanted MNCs.

Acknowledgments

This work was supported by the research grant for cardiovascular disease (16C-6) from the Ministry of Health, Labor and Welfare, Industrial Technology Research Grant Program in '03 from New Energy and Industrial Technology Development Organization (NEDO) of Japan, Health and Labor Sciences Research Grants-genome 005, the Mochida Memorial Foundation for Medical and Pharmaceutical Research, and the Promotion of Fundamental Studies in Health Science of the Organization for Pharmaceutical Safety and Research (OPSR) of Japan.

References

1. Belch JJ, Topol EJ, Agnelli G, et al. Critical issues in peripheral arterial disease detection and management: a call to action. *Arch Intern Med.* 2003;163:884–892.
2. Asahara T, Masuda H, Takahashi T, et al. Bone marrow origin of endothelial progenitor cells responsible for postnatal vasculogenesis in physiological and pathological neovascularization. *Circ Res.* 1999;85:221–228.
3. Shintani S, Murohara T, Ikeda H, et al. Augmentation of postnatal neovascularization with autologous bone marrow transplantation. *Circulation.* 2001;103:897–903.
4. Tateishi-Yuyama E, Matsubara H, Murohara T, et al. Therapeutic angiogenesis for patients with limb ischaemia by autologous transplantation of bone-marrow cells: a pilot study and a randomised controlled trial. *Lancet.* 2002;360:427–435.

5. Kitamura K, Kangawa K, Kawamoto M, et al. Adrenomedullin: a novel hypotensive peptide isolated from human pheochromocytoma. *Biochem Biophys Res Commun.* 1993;192:553–560.
6. Shindo T, Kurihara Y, Nishimatsu H, et al. Vascular abnormalities and elevated blood pressure in mice lacking adrenomedullin gene. *Circulation.* 2001;104:1964–1971.
7. Caron KM, Smithies O. Extreme hydrops fetalis and cardiovascular abnormalities in mice lacking a functional adrenomedullin gene. *Proc Natl Acad Sci U S A.* 2001;98:615–619.
8. Iimuro S, Shindo T, Moriyama N, et al. Angiogenic effects of adrenomedullin in ischemia and tumor growth. *Circ Res.* 2004;95:415–423.
9. Kim W, Moon SO, Sung MJ, et al. Protective effect of adrenomedullin in mannitol-induced apoptosis. *Apoptosis.* 2002;7:527–535.
10. Miyashita K, Itoh H, Sawada N, et al. Adrenomedullin provokes endothelial Akt activation and promotes vascular regeneration both in vitro and in vivo. *FEBS Lett.* 2003;544:86–92.
11. Murohara T, Ikeda H, Duan J, et al. Transplanted cord blood-derived endothelial precursor cells augment postnatal neovascularization. *J Clin Invest.* 2000;105:1527–1536.
12. Okumura H, Nagaya N, Itoh T, et al. Adrenomedullin infusion attenuates myocardial ischemia/reperfusion injury through the phosphatidylinositol 3-kinase/Akt-dependent pathway. *Circulation.* 2004;109:242–248.
13. Iwaguro H, Yamaguchi J, Kalka C, et al. Endothelial progenitor cell vascular endothelial growth factor gene transfer for vascular regeneration. *Circulation.* 2002;105:732–738.
14. Byrne MF, Corcoran PA, Atherton JC, et al. Stimulation of adhesion molecule expression by Helicobacter pylori and increased neutrophil adhesion to human umbilical vein endothelial cells. *FEBS Lett.* 2002;532:411–414.
15. Asahara T, Murohara T, Sullivan A, et al. Isolation of putative progenitor endothelial cells for angiogenesis. *Science.* 1997;275:964–967.
16. Nagaya N, Kangawa K, Kanda M, et al. Hybrid cell-gene therapy for pulmonary hypertension based on phagocytosing action of endothelial progenitor cells. *Circulation.* 2003;108:889–895.
17. Miura S, Matsuo Y, Saku K. Transactivation of KDR/Flk-1 by the B2 receptor induces tube formation in human coronary endothelial cells. *Hypertension.* 2003;41:1118–1123.
18. Tokunaga N, Nagaya N, Shirai M, et al. Adrenomedullin gene transfer induces therapeutic angiogenesis in a rabbit model of chronic hindlimb ischemia: benefits of a novel nonviral vector, gelatin. *Circulation.* 2004;109:526–531.
19. Iba O, Matsubara H, Nozawa Y, et al. Angiogenesis by implantation of peripheral blood mononuclear cells and platelets into ischemic limbs. *Circulation.* 2002;106:2019–2025.
20. Peled A, Grabovsky V, Habler L, et al. The chemokine SDF-1 stimulates integrin-mediated arrest of CD34(+) cells on vascular endothelium under shear flow. *J Clin Invest.* 1999;104:1199–1211.
21. Fujiyama S, Amano K, Uehira K, et al. Bone marrow monocyte lineage cells adhere on injured endothelium in a monocyte chemoattractant protein-1-dependent manner and accelerate reendothelialization as endothelial progenitor cells. *Circ Res.* 2003;93:980–989.
22. Asahara T, Takahashi T, Masuda H, et al. VEGF contributes to postnatal neovascularization by mobilizing bone marrow-derived endothelial progenitor cells. *EMBO J.* 1999;18:3964–3972.
23. Rissanen TT, Markkanen JE, Gruchala M, et al. VEGF-D is the strongest angiogenic and lymphangiogenic effector among VEGFs delivered into skeletal muscle via adenoviruses. *Circ Res.* 2003;92:1098–1106.
24. Nagaya N, Satoh T, Nishikimi T, et al. Hemodynamic, renal, and hormonal effects of adrenomedullin infusion in patients with congestive heart failure. *Circulation.* 2000;101:498–503.

□ CASE REPORT □

Primary Hyperparathyroidism Presumably Caused by Chronic Parathyroiditis Manifesting from Hypocalcemia to Severe Hypercalcemia

Sumiko FURUTO-KATO, Shigeru MATSUKURA, Makoto OGATA, Nobuyuki AZUMA, Toshiaki MANABE*, Chohei SHIGENO**, Ryo ASATO***, Kiyoshi TANAKA****, Yasato KOMATSU***** and Kazuwa NAKAO*****

Abstract

A 67-year-old woman who presented with hypocalcemia compatible with idiopathic hypoparathyroidism gradually changed into a state of primary hyperparathyroidism. The left upper parathyroid gland, which was larger and harder than other glands, was resected. Despite the operation, hypercalcemia and high levels of intact PTH persisted. Six weeks later total parathyroidectomy was done to induce remission. The resected gland in the first operation had clusters of lymphoid follicles with germinal centers indicating a chronic autoimmune inflammation. This case suggests a transition from hypoparathyroidim to hyperparathyroidism associated with chronic parathyroiditis, possibly by a mechanism analogous to that observed in chronic thyroiditis.
(Internal Medicine 44: 60–64, 2005)

Key words: hyperparathyroidism, chronic parathyroiditis, lymphoid follicles with germinal centers, hypercalcemia, hypocalcemia, Hashimoto's disease

Introduction

Primary hyperparathyroidism is generally caused by parathyroid adenoma, hyperplasia or occasionally carcinoma. The cause of hyperparathyroidism without the above lesions is sometimes difficult to identify. Regarding the pathology of the parathyroid gland, lymphoid follicles with germinal centers are rarely present in the parathyroid tissues. The presence of lymphoid follicles may indicate a chronic inflammatory process in the tissue. Bondeson et al (1) first reported two cases of chronic parathyroiditis associated with hyperparathyroidism. The possibility of hyperparathyroidism caused by autoimmunity in the parathyroid gland in the context of Graves' disease-like lymphoid infiltrate has been postulated. Since there was no evidence of underlying infections, a developmental anomaly, or drug reactions that could explain the inflammatory component, they suggested that an autoimmune process may have been involved in the pathogenesis (1). Chronic parathyroiditis itself has rarely been reported to date. Furthermore, cases manifesting severe hypocalcemia later changing to severe hypercalcemia associated with chronic parathyroiditis have not been reported to our knowledge. We report here a rare case of primary hyperparathyroidism which was presumably due to chronic parathyroiditis, which manifested from hypocalcemia to severe hypercalcemia.

Case Report

A 67-year-old woman saw a home doctor because of finger numbness in January 2000. She was referred to our hospital because plasma Ca levels were 6.4 mg/dl. When she visited our hospital on February 23, 2000, her plasma Ca and P levels were 7.2 mg/dl and 7.0 mg/dl, respectively. Plasma intact parathyroid hormone (PTH) was less than 9 pg/ml; the threshold of the assay. Her height was 159.2 cm, and her weight was 48.4 kg. Her blood pressure was 143/84 mmHg. In terms of family history her sister died of cerebral bleed-

From the Metabolism and Endocrinology Division of Internal Medicine, Kishiwada City Hospital, Osaka, *Department of Pathology, Kyoto University Graduate School of Medicine, Kyoto, **Department of Radiology, JT Kyoto Senbai Hospital, Kyoto, ***Department of Otolaryngology-Head and Neck Surgery, Kyoto University Graduate School of Medicine, Kyoto, ****Department of Nutrition, Kyoto Women University, Kyoto and *****Department of Medicine and Clinical Science, Kyoto University Graduate School of Medicine, Kyoto

Received for publication February 2, 2004; Accepted for publication August 17, 2004

Reprint requests should be addressed to Dr. Sumiko Furuto-Kato, the Metabolism and Endocrinology Division of Internal Medicine, Kishiwada City Hospital, 1001 Gakuhara-cho, Kishiwada, Osaka 596-8501

ing, and she had had lung tuberculosis at 10 years of age. Physical examination on admission showed Chvostek sign and Trousseau sign, although the finger numbness had already disappeared. Laboratory data on admission on March 23, 2000 are summarized in Table 1. The results of Ellsworth-Howard test were compatible with idiopathic hypoparathyroidism. Other basal levels of hormones, with the exception of PTH, were within normal limits. Treatment with 1α, 25-(OH)D_3 2 μg/day was initiated.

Table 1. Ca Related Data on First Admission

Plasma Ca	6.5 mg/dl (8.6–10.6)
Plasma P	6.9 mg/dl (2.5–4.8)
Plasma Mg	1.9 mg/dl (1.5–2.8)
Ionized Ca	1.68 mEq/l (2.41–2.71)
24h urine Ca	0.03 g
24h urine Mg	0.05 g
Intact-PTH	13 pg/ml (10–65)
HS-PTH	200 pg/ml (160–520)
C-PTH	0.2 ng/ml (<0.5)
1.25-$(OH)_2$ Vitamin D	45.7 pg/ml (20–60)

( ): normal range.

Plasma Ca and intact PTH gradually increased. The clinical course is shown in Fig. 1. Treatment with 1α, 25-$(OH)_2$ D_3 was slowly tapered, then terminated. On November 13, 2000, plasma Ca and also intact PTH levels continued to increase without any treatment. In March 2001, both plasma Ca and intact PTH were above the normal upper limits. According to these state of parathyroid function, the clinical diagnosis was changed to primary hyperparathyroidism. Plasma Ca and intact PTH still increased slowly and consistently over the next several months, and six months after the diagnosis of primary hyperparathyroidism, an acute increase in plasma Ca levels occurred, peaking from 14.7 mg/dl to 16.5 mg/dl in September 2001 (Fig. 1). The patient suffered from severe fatigue, appetite loss and body weight loss of 9 kg, compatible with parathyroid crisis. A series of tests including an ultrasound echogram, 99mTc-MIBI/I-123 subtraction scintigraphy, magnetic resonance imaging (MRI), and computed tomography (CT) of the neck and the chest could not provide any information regarding localization of the causative lesions. Plasma PTH-related protein (PTHrP)

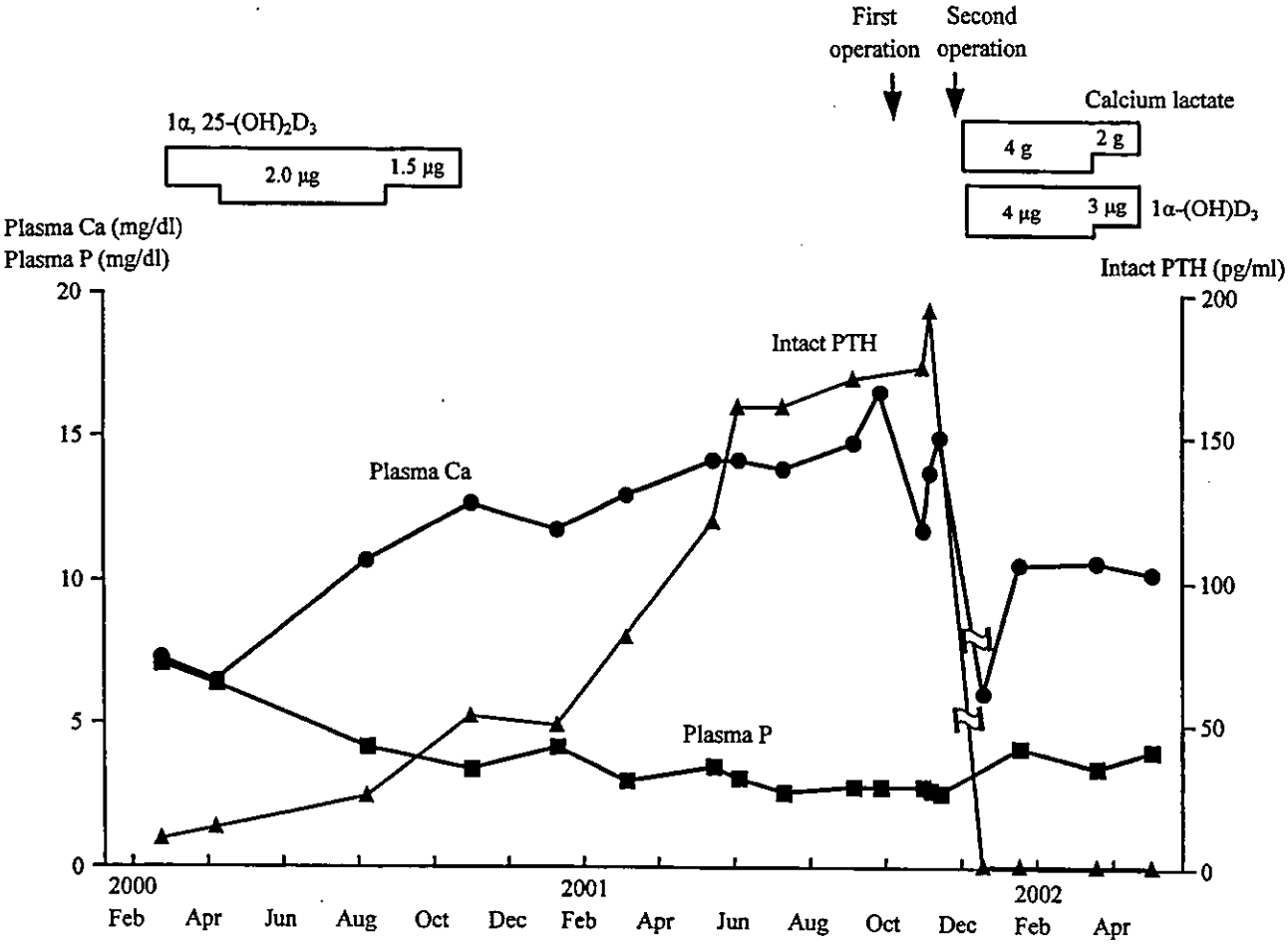

Figure 1. Clinical course of the patient.

Figure 2. Pathology of left superior parathyroid gland extirpated at the first operation demonstrating lymphoid follicles containing germinal centers.

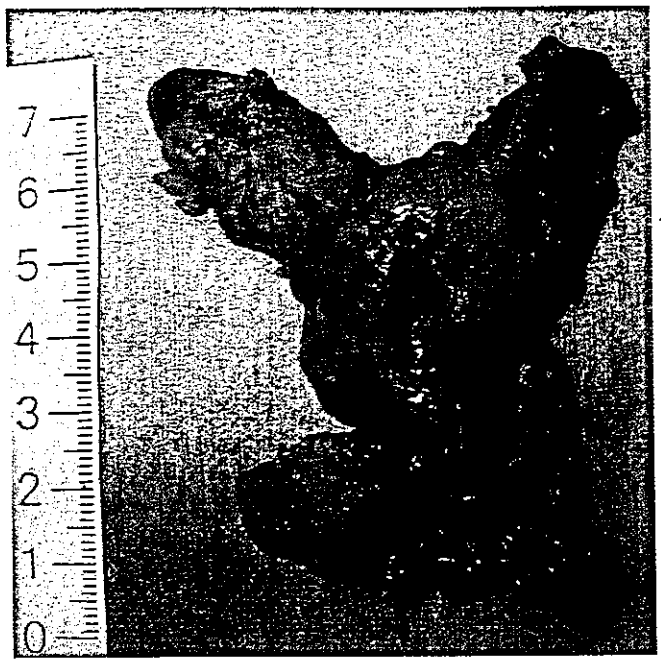

Figure 3. Resected specimens of the thyroid and fat tissue in the neck and superior thoracic region.

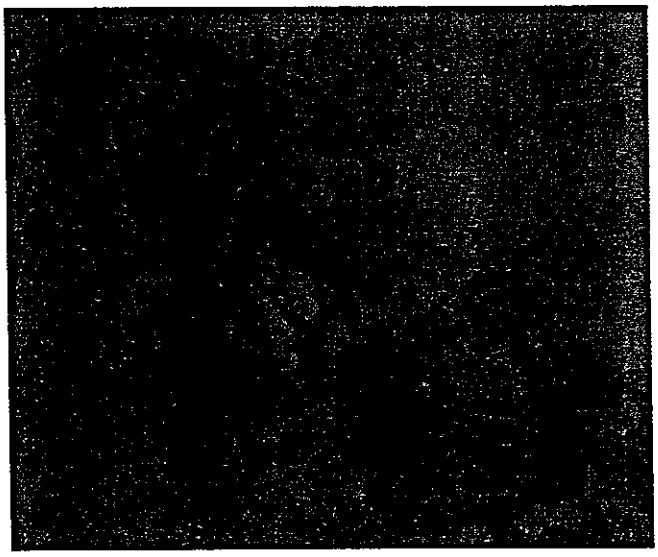

Figure 4. Pathology of the atrophic parathyroid gland resected at the second operation.

was within normal ranges. Antibodies against parathyroid gland and calcium-sensing receptor were not measured in the present study.

A parathyroidectomy was done on October 29, 2001. The left upper parathyroid gland, which was larger and harder than the other glands, was resected. Intrapoerative frozen section showed that it was compatible with the tumorous change. However, final detailed histological examination revealed that the resected gland was histologically almost normal and had infiltration of scattered lymphocytes and clusters of lymphoid follicles with germinal centers, indicating a chronic autoimmune inflammation (Fig. 2). Unfortunately, remission was not obtained after the operation. Venous sampling of the neck and the chest for intact PTH was performed. The levels of intact PTH were higher near the superior vena cava than the other regions. From this result, reoperation was elected.

After obtaining the informed consent, on December 7, 2001, total thyroidectomy and paratracheal neck-upper thoracic dissection (Fig. 3) were performed. After the operation, plasma Ca decreased and intact PTH was not detected: below the assay threshold. At present this state continues up, and 1α, 25-$(OH)_2D_3$ and thyroxine are given for replacement. With regard to the histology of the parathyroid glands, examinations of 4 mm slices identified the two additional parathyroid glands, that is, 1.8×0.7 mm in the tissue around the thyroid gland and 5 mm diameter in the paratracheal region. The former was atrophic (Fig. 4), and the latter was normal without any tumorous change and histologically there was focal infiltration of lymphcytes. Immunohistochemical staining for PTH was weakly positive in approximately 5% of the cells within the parathyroid gland resected at the first operation but the intensity of staining was weaker than that generally observed for normal parathyroid glands. Other glands resected at the second operation had been completely sliced thin, and thus no block was available for staining.

Discussion

The patient had clinical manifestations featuring a drastic change from hypocalcemia to hypercalcemia with pathological findings of lymphoid follicles with germinal centers in